
Coupled Gradient Flows for Strategic Non-Local Distribution Shift

Anonymous Author(s)

Affiliation

Address

email

Abstract

1 We propose a novel framework for analyzing the dynamics of distribution shift in
2 real-world systems that captures the feedback loop between learning algorithms and
3 the distributions on which they are deployed. Prior work largely models feedback-
4 induced distribution shift as adversarial or via an overly simplistic distribution-shift
5 structure. In contrast, we propose a coupled partial differential equation model that
6 captures fine-grained changes in the distribution over time by accounting for com-
7 plex dynamics that arise due to strategic responses to algorithmic decision-making,
8 non-local endogenous population interactions, and other exogenous sources of dis-
9 tribution shift. We consider two common settings in machine learning: cooperative
10 settings with information asymmetries, and competitive settings where a learner
11 faces strategic users. For both of these settings, when the algorithm retrains via
12 gradient descent, we prove asymptotic convergence of the retraining procedure to
13 a steady-state, both in finite and in infinite dimensions, obtaining explicit rates in
14 terms of the model parameters. To do so we derive new results on the convergence
15 of coupled PDEs that extends what is known on multi-species systems. Empirically,
16 we show that our approach captures well-documented forms of distribution shifts
17 like polarization and disparate impacts that simpler models cannot capture.

18 1 Introduction

19 In many machine learning tasks, there are commonly sources of exogenous and endogenous dis-
20 tribution shift, necessitating that the algorithm be retrained repeatedly over time. Some of these
21 shifts occur without the influence of an algorithm; for example, individuals influence each other to
22 become more or less similar in their attributes, or benign forms of distributional shift occur [Qui+].
23 Other shifts, however, are in response to algorithmic decision-making. Indeed, the very use of a
24 decision-making algorithm can incentivize individuals to change or mis-report their data to achieve
25 desired outcomes— a phenomenon known in economics as Goodhart’s law. Such phenomena have
26 been empirically observed, a well-known example being in [CC11], where researchers observed
27 a population in Columbia strategically mis-reporting data to game a poverty index score used for
28 distributing government assistance. Works such as [Mil+20; Wil+21], which investigate the effects of
29 distribution shift over time on a machine learning algorithm, point toward the need for evaluating the
30 robustness of algorithms to distribution shifts. Many existing approaches for modeling distribution
31 shift focus on simple metrics like optimizing over moments or covariates [DY10; LHL21; BBS09].
32 Other methods consider worst-case scenarios, as in distributionally robust optimization [AZ22;
33 LFG22; DN21; Kuh+19]. However, when humans respond to algorithms, these techniques may not
34 be sufficient to holistically capture the impact an algorithm has on a population. For example, an
35 algorithm that takes into account shifts in a distribution’s mean might inadvertently drive polarization,
36 rendering a portion of the population disadvantaged.

37 Motivated by the need for a more descriptive model, we present an alternative perspective which
 38 allows us to fully capture complex dynamics that might drive distribution shifts in real-world systems.
 39 Our approach is general enough to capture various sources of exogenous and endogenous distribution
 40 shift including the feedback loop between algorithms and data distributions studied in the literature on
 41 performative prediction [Per+20; IYZ21; Ray+22; Nar+22; MPZ21], the strategic interactions studied
 42 in strategic classification [Har+16; Don+18], and also endogenous factors like intra-population
 43 dynamics and distributional shifts. Indeed, while previous works have studied these phenomena in
 44 isolation, our method allows us to capture all of them as well as their interactions. For example,
 45 in [Zrn+21], the authors investigate the effects of dynamics in strategic classification problems—
 46 but the model they analyze does not capture individual interactions in the population. In [IYZ21],
 47 the authors model the interaction between a population that repeatedly responds to algorithmic
 48 decision-making by shifting its mean. Additionally, [Ray+22] study settings in which the population
 49 has both exogenous and endogenous distribution shifts due to feedback, but much like the other cited
 50 work, the focus remains on average performance. Each of these works fails to account for diffusion
 51 or intra-population interactions that can result in important qualitative changes to the distribution.

52 **Contributions.** Our approach to this problem relies on a detailed non-local PDE model of the data
 53 distribution which captures each of these factors. One term driving the evolution of the distribution
 54 over time captures the response of the population to the deployed algorithm, another draws on models
 55 used in the PDE literature for describing non-local effects and consensus in biological systems to
 56 model intra-population dynamics, and the last captures a background source of distribution shift.
 57 This is coupled with an ODE, lifted to a PDE, which describes the training of a machine learning
 58 algorithm results in a coupled PDE system which we analyze to better understand the behaviors that
 59 can arise among these interactions.

60 In one subcase, our model exhibits a joint gradient flow structure, where both PDEs can be written as
 61 gradients flows with respect to the same joint energy, but considering infinite dimensional gradients
 62 with respect to the different arguments. This mathematical structure provides powerful tools for
 63 analysis and has been an emerging area of study with a relatively small body of prior work, none of
 64 which related to distribution shifts in societal systems, and a general theory for multi-species gradient
 65 flows is still lacking. We give a brief overview of the models that are known to exhibit this joint
 66 gradient flow structure: in [DS20] the authors consider a two-species tumor model with coupling
 67 through Brinkman’s Law. A number of works consider coupling via convolution kernels [Bur+18;
 68 Giu+22; JPZ22; CHS18; FF13; FF13; DT20] and cross-diffusion [LY22; AB21; MKB14], with
 69 applications in chemotaxis among other areas. In the models we consider here, the way the interaction
 70 between the two populations manifests is neither via cross-diffusion, nor via the non-local interaction
 71 term. It represents a new way of coupling the evolution of two interacting species via gradient flows
 72 and our results on the long-time asymptotics for these coupled PDEs add to the current state-of-the-art
 73 in the field. In the other subcase, we prove exponential convergence in two competitive, timescale
 74 separated settings where the algorithm and strategic population have conflicting objectives. We show
 75 numerically that retraining in a competitive setting leads to polarization in the population, illustrating
 76 the importance of fine-grained modeling.

77 2 Problem Formulation

78 Machine learning algorithms that are deployed into the real world for decision-making often become
 79 part of complex feedback loops with the data distributions and data sources with which they interact.
 80 In an effort to model these interactions, consider a machine learning algorithm that has loss given by
 81 $L(z, x)$ where $x \in \mathbb{R}^d$ are the algorithm parameters and $z \in \mathbb{R}^d$ are the population attributes, and the
 82 goal is to solve

$$\operatorname{argmin}_{x \in \mathcal{X}} \mathbb{E}_{z \sim \rho} L(z, x),$$

83 where \mathcal{X} is the class of model parameters and $\rho(z)$ is the population distribution. Individuals have an
 84 objective given by $J(z, x)$ in response to a model parameterized by x , and they seek to solve

$$\operatorname{argmin}_{z \in \mathbb{R}^d} \mathbb{E}_{z \sim \rho} J(z, x).$$

85 When individuals in the population and the algorithm have access to gradients, we model the
 86 optimization process as a gradient-descent-type process. Realistically, individuals in the population

87 will have nonlocal information and influences, as well as external perturbations, the effects of
 88 which we seek to capture in addition to just minimization. To address this, we propose a partial
 89 differential equation (PDE) model for the population, that while modelling the individuals as a
 90 collective population, also maintains the nonlocal interactions of individuals. The model for this
 91 strategic population population is given by

$$\partial_t \rho = \operatorname{div} \left(\rho \nabla \delta_\rho \left[\mathbb{E}_{z \sim \rho} J(z, x) + E(\rho) \right] \right), \quad (1)$$

92 where $E(\rho)$ is a functional with terms for influences and external perturbations. In real-world
 93 deployment of algorithms, decision makers update their algorithm over time, leading to an interaction
 94 between the two processes. We also consider the algorithm dynamics over time, which we model as

$$\dot{x} = -\nabla_x \left[\mathbb{E}_{z \sim \rho} L(z, x) \right]. \quad (2)$$

95 In this work, we analyze the behavior of the dynamics under the following model. The algorithm
 96 suffers a cost $f_1(z, x)$ for a data point z under model parameters x in the strategic population, and a
 97 cost $f_2(z, x)$ for a data point in a fixed, non-strategic population. The strategic population is denoted
 98 by $\rho \in \mathcal{P}$, and the non-strategic $\bar{\rho} \in \mathcal{P}$, where \mathcal{P} is the space of probability measures on the Borel
 99 sigma algebra. The algorithm aims to minimize

$$\mathbb{E}_{z \sim \rho} L(z, x) = \int f_1(z, x) d\rho(z) + \int f_2(z, x) d\bar{\rho}(z) + \frac{\beta}{2} \|x - x_0\|^2,$$

100 where the norm is the vector inner product $\|x\|^2 = \langle x, x \rangle$ and $\beta > 0$ weighs the cost of updating the
 101 model parameters from its initial condition.

102 We consider two settings: (i) aligned objectives, and (ii) competing objectives. Case (i) captures the
 103 setting in which the strategic population minimization improves the performance of the algorithm,
 104 subject to a cost for deviating from a reference distribution $\bar{\rho} \in \mathcal{P}$. This cost stems from effort
 105 required to manipulate features, such as a loan applicant adding or closing credit cards. On the
 106 other hand, Case (ii) captures the setting in which the strategic population minimization worsens the
 107 performance of the algorithm, again incurring cost from distributional changes.

108 2.1 Case (i): Aligned Objectives

109 In this setting, we consider the case where the strategic population and the algorithm have aligned
 110 objectives. This occurs in examples such as recommendation systems, where users and algorithm
 111 designers both seek to develop accurate recommendations for the users. This corresponds to the
 112 population cost

$$\mathbb{E}_{z \sim \rho, x \sim \mu} J(z, x) = \iint f_1(z, x) d\rho(z) d\mu(x) + \alpha KL(\rho | \bar{\rho}),$$

113 where $KL(\cdot | \cdot)$ denotes the Kullback-Leibler divergence. Note that the KL divergence introduces
 114 diffusion to the dynamics for ρ . The weight $\alpha > 0$ parameterizes the cost of distribution shift to the
 115 population. To account for nonlocal information and influence among members of the population,
 116 we include a kernel term $E(\rho) = \frac{1}{2} \int \rho W * \rho dz$, where $W * \rho$ is a convolution integral and W is a
 117 suitable interaction potential.

118 2.2 Case (ii): Competing Objectives

119 In settings such as online internet forums, where algorithms and users have used manipulative
 120 strategies for marketing [Del06], the strategic population may be incentivized to modify or mis-report
 121 their attributes. The algorithm has a competitive objective, in that it aims to maintain performance
 122 against a population whose dynamics cause the algorithm performance to suffer. When the strategic
 123 population seeks an outcome contrary to the algorithm, we model strategic population cost as

$$\mathbb{E}_{z \sim \rho, x \sim \mu} J(z, x) = - \iint f_1(z, x) d\rho(z) d\mu(x) + \alpha KL(\rho | \bar{\rho}).$$

124 A significant factor in the dynamics for the strategic population is the timescale separation between
 125 the two "species"—i.e., the population and the algorithm. In our analysis, we will consider two cases:
 126 one, where the population responds much faster than the algorithm, and two, where the algorithm
 127 responds much faster than the population. We illustrate the intermediate case in a simulation example.

128 **3 Results**

129 We are interested in characterizing the long-time asymptotic behavior of the population distribution,
 130 as it depends on the decision-makers action over time. The structure of the population distribution
 131 gives us insights about how the decision-makers actions influences the entire population of users.
 132 For instance, as noted in the preceding sections, different behaviors such as bimodal distributions or
 133 large tails or variance might emerge, and such effects are not captured in simply looking at average
 134 performance. To understand this intricate interplay, one would like to characterize the behavior of
 135 both the population and the algorithm over large times. Our main contribution towards this goal is a
 136 novel analytical framework as well as analysis of the long-time asymptotics.

137 A key observation is that the dynamics in (1) and (2) can be re-formulated as a gradient flow; we lift
 138 x to a probability distribution μ by representing it as a Dirac delta μ sitting at the point x . As a result,
 139 the evolution of μ will be governed by a PDE, and combined with the PDE for the population, we
 140 obtain a system of coupled PDEs,

$$\begin{aligned}\partial_t \rho &= \operatorname{div} \left(\rho \nabla_z \delta_\rho \left[\mathbb{E}_{z \sim \rho, x \sim \mu} J(z, x) + E(\rho) \right] \right) \\ \partial_t \mu &= \operatorname{div} \left(\mu \nabla_x \delta_\mu \left[\mathbb{E}_{z \sim \rho, x \sim \mu} L(z, x) \right] \right),\end{aligned}$$

141 where δ_ρ and δ_μ are first variations with respect to ρ and μ according to Definition A.2. The natural
 142 candidates for the asymptotic profiles of this coupled system are its steady states, which - thanks
 143 to the gradient flow structure - can be characterized as ground states of the corresponding energy
 144 functionals. In this work, we show existence and uniqueness of minimizers (maximizers) for the
 145 functionals under suitable conditions on the dynamics. We also provide criteria for convergence and
 146 explicit convergence rates. We begin with the case where the interests of the population and algorithm
 147 are aligned, and follow with analogous results in the competitive setting. We show convergence
 148 energy, which ensures convergence in a product Wasserstein metric. For convergence in energy, we
 149 use the notion of relative energy and prove that the relative energy converges to zero as time increases.
 150

151 **Definition 1 (Relative Energy).** *The relative energy of a functional G is given by $G(\gamma|\gamma_\infty) =$
 152 $G(\gamma) - G(\gamma_\infty)$, where $G(\gamma_\infty)$ is the energy at the steady state.*

153 Since we consider the joint evolution of two probability distributions, we define a distance metric
 154 \overline{W} on the product space of probability measures with bounded second moment. We will establish
 155 convergence both in energy and in the metric \overline{W} .

156 **Definition 2 (Joint Wasserstein Metric).** *The metric over $\mathcal{P}_2 \times \mathcal{P}_2$ is called \overline{W} and is given by*

$$\overline{W}((\rho, \mu), (\tilde{\rho}, \tilde{\mu}))^2 = W_2(\rho, \tilde{\rho})^2 + W_2(\mu, \tilde{\mu})^2$$

157 *for all pairs $(\rho, \mu), (\tilde{\rho}, \tilde{\mu}) \in \mathcal{P}_2(\mathbb{R}^d) \times \mathcal{P}_2(\mathbb{R}^d)$, and where W_2 denotes the Wasserstein-2 metric (see*
 158 *Definition 3). We denote by $\overline{W}(\mathbb{R}^d) := (\mathcal{P}_2(\mathbb{R}^d) \times \mathcal{P}_2(\mathbb{R}^d), \overline{W})$ the corresponding metric space.*

159 **3.1 Gradient Flow Structure**

160 In the case where the objectives of the algorithm and population are aligned, we can write the
 161 dynamics as a gradient flow by using the same energy functional for both species. Let $G_a(\rho, \mu) :$
 162 $\mathcal{P}(\mathbb{R}^d) \times \mathcal{P}(\mathbb{R}^d) \mapsto [0, \infty]$ be the energy functional given by

$$\begin{aligned}G_a(\rho, \mu) &= \iint f_1(z, x) d\rho(z) d\mu(x) + \iint f_2(z, x) d\tilde{\rho}(z) d\mu(x) + \alpha KL(\rho|\tilde{\rho}) + \frac{1}{2} \int \rho W * \rho \\ &\quad + \frac{\beta}{2} \int \|x - x_0\|^2 d\mu(x).\end{aligned}$$

163 This expression is well-defined as the relative entropy $KL(\rho|\tilde{\rho})$ can be extended to the full set
 164 $\mathcal{P}(\mathbb{R}^d)$ by setting $G_a(\rho, \mu) = +\infty$ in case ρ is not absolutely continuous with respect to $\tilde{\rho}$.

165 In the competitive case we define $G_c(\rho, x) : \mathcal{P}(\mathbb{R}^d) \times \mathbb{R}^d \mapsto [-\infty, \infty]$ by

$$G_c(\rho, x) = \int f_1(z, x) d\rho(z) + \int f_2(x, z') d\tilde{\rho}(z') - \alpha KL(\rho|\tilde{\rho}) - \frac{1}{2} \int \rho W * \rho + \frac{\beta}{2} \|x - x_0\|^2.$$

166 In settings like recommender systems, the population and algorithm have aligned objectives; they
 167 seek to minimize the same cost but are subject to different dynamic constraints and influences,
 168 modeled by the regularizer and convolution terms. In the case where the objectives are aligned, the
 169 dynamics are given by

$$\begin{aligned}\partial_t \rho &= \operatorname{div}(\rho \nabla_z \delta_\rho G_a[\rho, \mu]) \\ \partial_t \mu &= \operatorname{div}(\mu \nabla_x \delta_\mu G_a[\rho, \mu]).\end{aligned}\tag{3}$$

170 Note that (3) is a joint gradient flow, because the dynamics can be written in the form $\partial_t \gamma =$
 171 $\operatorname{div}(\gamma \nabla \delta_\gamma G_a(\gamma))$, where $\gamma = (\rho, \mu)$ and where the gradient and divergence are taken in both
 172 variables (z, x) .

173 In other settings, such as credit score reporting, the objectives of the population are competitive with
 174 the algorithm. Here we consider two scenarios; one, where the algorithm responds quickly relative
 175 to the population, and two, where the population responds quickly relative to the algorithm. In the
 176 case where the algorithm can immediately adjust optimally (best-respond) to the distribution, the
 177 dynamics are given by

$$\begin{aligned}\partial_t \rho &= -\operatorname{div}(\rho (\nabla_z \delta_\rho G_c[\rho, x])|_{x=b(\rho)}), \\ b(\rho) &:= \operatorname{argmin}_{\bar{x}} G_c(\rho, \bar{x}).\end{aligned}\tag{4}$$

178 Next we can consider the population immediately responding to the algorithm, which has dynamics

$$\begin{aligned}\frac{d}{dt} x &= -\nabla_x G_c(\rho, x)|_{\rho=r(x)}, \\ r(x) &:= \operatorname{argmin}_{\hat{\rho} \in \mathcal{P}} -G_c(\hat{\rho}, x).\end{aligned}\tag{5}$$

179 The key results on existence and uniqueness of a ground state as well as the convergence behavior
 180 of solutions depend on convexity (concavity) of G_a and G_c . The notion of convexity that we will
 181 employ for energy functionals is *(uniform) displacement convexity*, which is analogous to (strong)
 182 convexity in Euclidean spaces. One can think of displacement convexity for an energy functional
 183 defined on \mathcal{P}_2 as convexity along the shortest path in the Wasserstein-2 metric (linear interpolation in
 184 the Wasserstein-2 space) between any two given probability distributions. For a detailed definition
 185 of (uniform) displacement convexity and concavity, see Section A.2. In fact, suitable convexity
 186 properties of the input functions f_1, f_2 and $\tilde{\rho}$ will ensure (uniform) displacement convexity of the
 187 resulting energy functionals appearing in the gradient flow structure, see for instance [Vil03b, Chapter
 188 5.2].

189 We make the following assumptions in both the competitive case and aligned interest cases. Here,
 190 I_d denotes the $d \times d$ identity matrix, $\operatorname{Hess}(f)$ denotes the Hessian of f in all variables, while $\nabla_x^2 f$
 191 denotes the Hessian of f in the variable x only.

192 **Assumption 1** (Convexity of f_1 and f_2). *The functions $f_1, f_2 \in C^2(\mathbb{R}^d \times \mathbb{R}^d; [0, \infty))$ satisfy for all*
 193 $(z, x) \in \mathbb{R}^d \times \mathbb{R}^d$ *the following:*

- 194 • *There exists constants $\lambda_1, \lambda_2 \geq 0$ such that $\operatorname{Hess}(f_1) \succeq \lambda_1 I_{2d}$ and $\nabla_x^2 f_2 \succeq \lambda_2 I_d$;*
- 195 • *There exist constants $a_i > 0$ such that $x \cdot \nabla_x f_i(z, x) \geq -a_i$ for $i = 1, 2$;*
- 196 • *There exists a constant $\sigma \geq 0$ such that $\|\nabla_x \nabla_x f_1(z, x)\| \leq \sigma$.*

197 **Assumption 2** (Reference Distribution Shape). *The reference distribution $\tilde{\rho} \in \mathcal{P}(\mathbb{R}^d) \cap L^1(\mathbb{R}^d)$*
 198 *satisfies $\log \tilde{\rho} \in C^2(\mathbb{R}^d)$ and $\nabla_z^2 \log \tilde{\rho}(z) \preceq -\tilde{\lambda} I_d$ for some $\tilde{\lambda} > 0$.*

199 **Assumption 3** (Convex Interaction Kernel). *The interaction kernel $W \in C^2(\mathbb{R}^d; [0, \infty))$ is convex,*
 200 *symmetric $W(-z) = W(z)$, and for some $D > 0$ satisfies*

$$z \cdot \nabla_z W(z) \geq -D, \quad |\nabla_z W(z)| \leq D(1 + |z|) \quad \forall z \in \mathbb{R}^d.$$

201 We make the following observations regarding the assumptions above:

- 202 • *The convexity in Assumption 3 can be relaxed and without affecting the results outlined*
 203 *below by following a more detailed analysis analogous to the approach in [CMV03].*
- 204 • *If f_1 and f_2 are strongly convex, the proveable convergence rate increases, but without strict*
 205 *or strong convexity of f_1 and f_2 , the regularizers $KL(\rho|\tilde{\rho})$ and $\int \|x - x_0\|_2^2 dx$ provide the*
 206 *convexity guarantees necessary for convergence.*

207 For concreteness, one can consider the following classical choices of input functions to the evolution:

- 208 • Using the log-loss function for f_1 and f_2 satisfies Assumption 1.
- 209 • Taking the reference measure $\tilde{\rho}$ to be the normal distribution satisfies Assumption 2, which
- 210 ensures the distribution is not too flat.
- 211 • Taking quadratic interactions $W(z) = \frac{1}{2}|z|^2$ satisfies Assumption 3.

212 **Remark 1** (Cauchy-Problem). *To complete the arguments on convergence to equilibrium, we require*
 213 *sufficient regularity of solutions to the PDEs under consideration. In fact, it is sufficient if we can*
 214 *show that equations (3), (4), and (5) can be approximated by equations with smooth solutions. Albeit*
 215 *tedious, these are standard techniques in the regularity theory for partial differential equations,*
 216 *see for example [CMV03, Proposition 2.1 and Appendix A], [OV00], [Vil03b, Chapter 9], and the*
 217 *references therein. Similar arguments as in [DV00] are expected to apply to the coupled gradient*
 218 *flows considered here, guaranteeing existence of smooth solutions with fast enough decay at infinity,*
 219 *and we leave a detailed proof for future work.*

220 3.2 Analysis of Case (i): Aligned Objectives

221 The primary technical contribution of this setting consists of lifting the algorithm dynamics from an
 222 ODE to a PDE, which allows us to model the system as a joint gradient flow on the product space of
 223 probability measures. The coupling occurs in the potential function, rather than as cross-diffusion or
 224 non-local interaction as previously seen in the literature for multi-species systems.

225 **Theorem 1.** *Suppose that Assumptions 1-3 are satisfied and let $\eta := \lambda_1 + \min(\lambda_2 + \beta, \alpha\tilde{\lambda}) > 0$.*
 226 *Consider solutions $\gamma_t := (\rho_t, \mu_t)$ to the dynamics (3) with initial conditions satisfying $\gamma_0 \in \mathcal{P}_2(\mathbb{R}^d) \times$*
 227 *$\mathcal{P}_2(\mathbb{R}^d)$ and $G_a(\gamma_0) < \infty$. Then the following hold:*

228 (a) *There exists a unique minimizer γ_∞ of G_a , which is also the unique steady state for equation*
 229 *(3).*

230 (b) *The solution γ_t converges exponentially fast in G_a and \overline{W} ,*

$$G_a(\gamma_t | \gamma_\infty) \leq e^{-2\eta t} G_a(\gamma_0 | \gamma_\infty) \quad \text{and} \quad \overline{W}(\gamma_t, \gamma_\infty) \leq ce^{-\eta t} \quad \text{for all } t \geq 0,$$

231 *where $c > 0$ is a constant only depending on γ_0, γ_∞ and the parameter η .*

232 *Proof.* (Sketch) For existence and uniqueness, we leverage classical techniques in the calculus
 233 of variations. To obtain convergence to equilibrium in energy, our key result is a new HWI-type
 234 inequality, providing as a consequence generalizations of the log-Sobolev inequality and the Talagrand
 235 inequality. Together, these inequalities relate the energy (classically denoted by H in the case of the
 236 Boltzmann entropy), the metric (classically denoted by W in the case of the Wasserstein-2 metric) and
 237 the energy dissipation (classically denoted by I in the case of the Fisher information)¹. Combining
 238 these inequalities with Gronwall's inequality allows us to deduce convergence both in energy and in
 239 the metric \overline{W} . □

240 3.3 Analysis of Case (ii): Competing Objectives

241 In this setting, we consider the case where the algorithm and the strategic population have goals in
 242 opposition to each other; specifically, the population benefits from being classified incorrectly. First,
 243 we will show that when the algorithm instantly best-responds to the population, then the distribution
 244 of the population converges exponentially in energy and in W_2 . Then we will show a similar result
 245 for the case where the population instantly best-responds to the algorithm.

246 In both cases, we begin by proving two Danskin-type results (see [Dan67; Ber71]) which will be used
 247 for the main convergence theorem, including convexity (concavity) results. To this end, we make the
 248 following assumption ensuring that the regularizing component in the evolution of ρ is able to control
 249 the convexity introduced by f_1 and f_2 .

250 **Assumption 4** (Upper bounds for f_1 and f_2). *There exists a constant $\Lambda_1 > 0$ such that*

$$\nabla_z^2 f_1(z, x) \preceq \Lambda_1 I_d \quad \text{for all } (z, x) \in \mathbb{R}^d \times \mathbb{R}^d.$$

¹Hence the name HWI inequalities.

251 and for any $R > 0$ there exists a constant $c_2 \in \mathbb{R}$ such that

$$\sup_{x \in B_R(0)} \int f_2(z, x) d\bar{\rho}(z) < c_2.$$

252 Equipped with Assumption 4, we state the result for a best-responding algorithm.

253 **Theorem 2.** *Suppose Assumptions 1-4 are satisfied with $\alpha\tilde{\lambda} > \Lambda_1$. Let $\lambda_b := \alpha\tilde{\lambda} - \Lambda_1$. Define*
 254 $G_b(\rho) := G_c(\rho, b(\rho))$. *Consider a solution ρ_t to the dynamics (4) with initial condition $\rho_0 \in \mathcal{P}_2(\mathbb{R}^d)$*
 255 *such that $G_b(\rho_0) < \infty$. Then the following hold:*

256 (a) *There exists a unique maximizer ρ_∞ of $G_b(\rho)$ which is also the unique steady state of (4).*

257 (b) *The solution ρ_t converges exponentially fast to ρ_∞ with rate λ_b in $G_b(\cdot | \rho_\infty)$ and W_2 ,*

$$G_b(\rho_t | \rho_\infty) \leq e^{-2\lambda_b t} G_a(\rho_0 | \rho_\infty) \quad \text{and} \quad W_2(\rho_t, \rho_\infty) \leq ce^{-\lambda_b t} \quad \text{for all } t \geq 0,$$

258 *where $c > 0$ is a constant only depending on ρ_0 , ρ_∞ and the parameter λ_b .*

259 *Proof.* (Sketch) The key addition in this setting as compared with Theorem 1 is proving that $G_b(\rho)$
 260 is bounded below, uniformly displacement concave and guaranteeing its smoothness via Berge's
 261 Maximum Theorem. This is non-trivial as it uses the properties of the best response $b(\rho)$. A central
 262 observation for our arguments to work is that $\delta_\rho G_b[\rho] = (\delta_\rho G_c[\rho, x])|_{x=b(\rho)}$. We can then conclude
 263 using the direct method in the calculus of variations and the HWI method. \square

264 Here, the condition that $\alpha\tilde{\lambda}$ must be large enough corresponds to the statement that the system must
 265 be subjected to a strong enough regularizing effect.

266 In the opposite case, where ρ instantly best-responds to the algorithm, we show Danskin-like results
 267 for derivatives through the best response function and convexity of the resulting energy in x which
 268 allows to deduce convergence.

269 **Theorem 3.** *Suppose Assumptions 1-4 are satisfied. Define $G_d(x) := G_c(r(x), x)$. Then it holds:*

270 (a) *There exists a unique minimizer x_∞ of $G_d(x)$.*

271 (b) *The vector $x(t)$ solving the dynamics (5) with initial condition $x(0) \in \mathbb{R}^d$ converges*
 272 *exponentially fast to x_∞ with rate $\lambda_d := \lambda_1 + \lambda_2 + \beta > 0$ in G_d and in the Euclidean norm:*

$$\begin{aligned} \|x(t) - x_\infty\| &\leq e^{-\lambda_d t} \|x(0) - x_\infty\|, \\ G_d(x(t)) - G_d(x_\infty) &\leq e^{-2\lambda_d t} (G_d(x(0)) - G_d(x_\infty)) \end{aligned}$$

273 *for all $t \geq 0$.*

274 These two theorems illustrate that, under sufficient convexity conditions on the cost functions, we
 275 expect the distribution ρ and the algorithm x to converge to a steady state. In practice, when the
 276 distributions are close enough to the steady state there is no need to retrain the algorithm.

277 While we have proven results for the extreme timescale cases, we anticipate convergence to the same
 278 equilibrium in the intermediate cases. Indeed, it is well known (especially for systems in Euclidean
 279 space) that two-timescale stochastic approximation dynamical systems, with appropriate stepsize
 280 choices, converge asymptotically, and finite-time high probability concentration bounds can also
 281 be obtained [Bor09]. These results have been leveraged in strategic classification [Zrn+21], and
 282 Stackelberg games [FCR20; FR21; Fie+21]. We leave this intricate analysis to future work.

283 In the following section we show numerical results in the case of a best-responding x , best-responding
 284 ρ , and in between where x and ρ evolve on a similar timescale. Note that in these settings, the
 285 dynamics do not have a gradient flow structure due to a sign difference in the energies, requiring
 286 conditions to ensure that one species does not dominate the other.

287 4 Numerical Examples

288 We illustrate numerical results for the case of a classifier, which are used in scenarios such as loan
 289 or government aid applications [CC11], school admissions [PS13], residency match [Ree18], and
 290 recommendation algorithms [LSW10], all of which have some population which is incentivized

291 to submit data that will result in a desirable classification. For all examples, we select classifiers
 292 of the form $x \in \mathbb{R}$, so that a data point $z \in \mathbb{R}$ is assigned a label of 1 with probability $q(z, x) =$
 293 $(1 + \exp(-b^\top z + x))^{-1}$ where $b > 0$. Let f_1 and f_2 be given by

$$f_1(z, x) = -\log(1 - q(z, x)), \quad f_2(z, x) = -\log q(z, x).$$

294 Note that $\text{Hess}(f_1) \succeq 0$ and $\text{Hess}(f_2) \succeq$, so $\lambda_1 = \lambda_2 = 0$. The strictness of the convexity of the
 295 functional is coming from the regularizers, not the cost functions. We show numerical results for two
 296 scenarios with additional settings in the appendix. First we illustrate competitive interests under three
 297 different timescale settings. Then we simulate the classifier taking an even more naïve strategy than
 298 gradient descent and discuss the results. The PDEs were implemented based on the finite volume
 299 method from [CCH15].

300 4.1 Competitive Objectives

301 In the setting with competitive objectives, we utilize $G_c(\rho, x)$ with $W = 0$, f_1 and f_2 as defined
 302 above with $b = 3$ fixed as it only changes the steepness of the classifier for $d = 1$, and $\alpha = 0.1$ and
 303 $\beta = 0.05$. In Figure 1, we simulate two extremes of the timescale setting; first when ρ is nearly
 304 best-responding and then when x is best-responding. The simulations have the same initial conditions
 305 and end with the same distribution shape; however, the behavior of the strategic population differs in
 the intermediate stages. When ρ is nearly best-responding, we see that the distribution quickly shifts

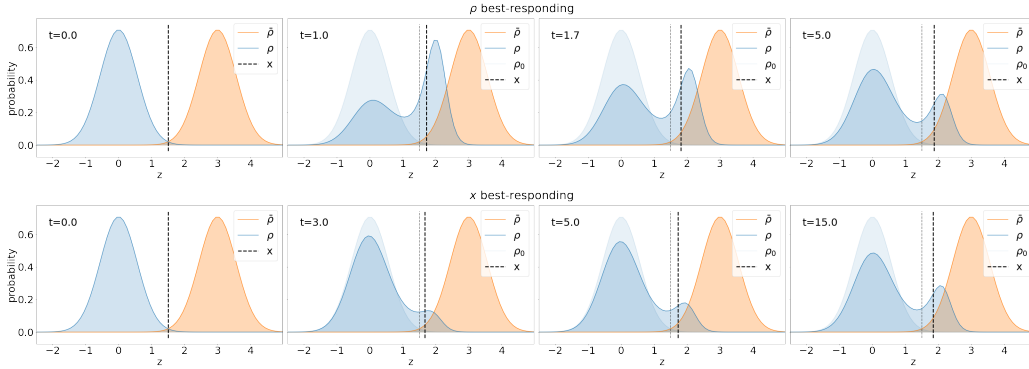


Figure 1: When x versus ρ best-responds, we observe the same final state but different intermediate states. Modes appear in the strategic population which simpler models cannot capture.

306 mass over the classifier threshold. Then the classifier shifts right, correcting for the shift in ρ , which
 307 then incentivizes ρ to shift more mass back to the original mode. In contrast, when x best-responds,
 308 the right-hand mode slowly increases in size until the system converges.
 309

310 Figure 2 shows simulation results from the setting where ρ and x evolve on the same timescale. We
 311 observe that the distribution shift in ρ appears to fall between the two extreme timescale cases, which
 we expect. We highlight two important observations for the competitive case. One, a single-mode

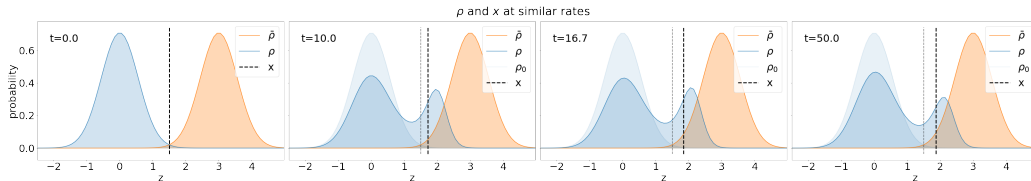


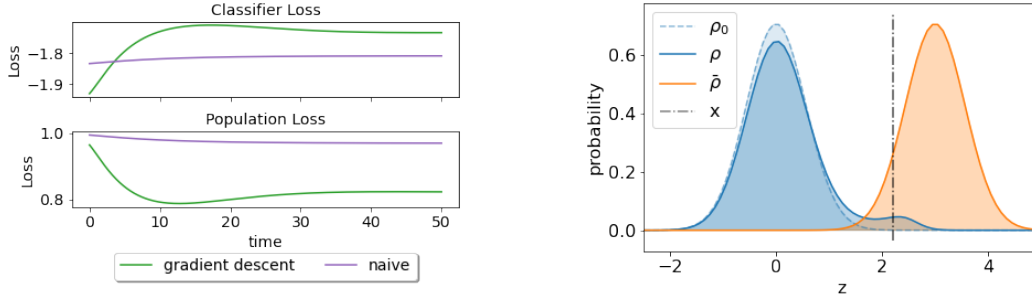
Figure 2: In this experiment the population and classifier have similar rates of change, and the distribution change for ρ exhibits behaviors from both the fast ρ and fast x simulations; the right-hand mode does not peak as high as the fast ρ case but does exceed its final height and return to the equilibrium.

312 distribution becomes bimodal, which would not be captured using simplistic metrics such as the
 313 mean and variance. This split can be seen as polarization in the population, a phenomenon that
 314

315 a mean-based strategic classification model would not capture. Two, the timescale on which the
 316 classifier updates significantly impacts the intermediate behavior of the distribution. In our example,
 317 when x updated slowly relative to the strategic population, the shifts in the population were greater
 318 than in the other two cases. This suggests that understanding the effects of timescale separation are
 319 important for minimizing volatility of the coupled dynamics.

320 4.2 Naïve Behavior

321 In this example, we explore the results of the classifier adopting a non-gradient-flow strategy, where
 322 the classifier chooses an initially-suboptimal value for x and does not move, allowing the strategic
 population to respond. All functions and parameters are the same as in the previous example. When



(a) Both species minimize their respective losses; when the classifier uses a naïve strategy, the final performance is better for the classifier and uniformly worse for the population.

(b) The classifier selects a suboptimal initial condition $x = 2.2$, instead of $x = 1.5$ which minimizes the initial loss, and then does not move in response to the population.

Figure 3: Although the classifier starts with a larger cost by taking the naïve strategy, the final loss is better. This illustrates how our model can be used to compare robustness of different strategies against a strategic population.

323 comparing with the gradient descent strategy, we observe that while the initial loss for the classifier
 324 is worse for the naïve strategy, the final cost is better. While this results is not surprising, because
 325 one can view this as a general-sum game where the best response to a fixed decision may be better
 326 than the equilibrium, it illustrates how our method provides a framework for evaluating how different
 327 training strategies perform in the long run against a strategic population.
 328

329 5 Future Directions, Limitations, and Broader Impact

330 Our work presents a method for evaluating the robustness of an algorithm to a strategic population,
 331 and investigating a variety of robustness using our techniques opens a range of future research
 332 directions. Additionally, our application suggests many questions relevant to the PDE literature, such
 333 as: (1) Does convergence still hold with the gradient replaced by an estimated gradient? (2) Can we
 334 prove convergence in between the two timescale extremes? (3) How do multiple dynamic populations
 335 respond to an algorithm, or multiple algorithms?

336 A challenge in our method is that numerically solving high-dimensional PDEs is computationally
 337 expensive and possibly unfeasible. Here we note that in many applications, agents in the population
 338 do not alter more than a few features due to the cost of manipulation. We are encouraged by the
 339 recent progress using deep learning to solve PDEs, which could be used in our application.

340 **Broader Impacts** Modeling the full population distribution rather than simple metrics of the distri-
 341 bution is important because not all individuals are affected by the algorithm in the same way. For
 342 example, if there are tails of the distribution that have poor performance even if on average the model
 343 is good, we need to know how that group is advantaged or disadvantaged relative to the rest of the
 344 population. Additionally, understanding how people respond to algorithms offers an opportunity to
 345 incentivise people to move in a direction that increases social welfare.

346 **References**

- 347 [Ala40] Leon Alaoglu. “Weak Topologies of Normed Linear Spaces”. In: *The Annals of Mathe-*
348 *matics* 41.1 (Jan. 1940), p. 252. ISSN: 0003486X. DOI: 10.2307/1968829. URL: <https://www.jstor.org/stable/1968829?origin=crossref> (visited on 05/24/2023).
- 350 [Dan67] John M. Danskin. *The Theory of Max-Min and its Application to Weapons Al-*
351 *location Problems*. Red. by M. Beckmann et al. Vol. 5. *Ä-konometrie und Un-*
352 *ternehmensforschung / Econometrics and Operations Research*. Berlin, Heidelberg:
353 Springer, 1967. ISBN: 9783642460944 9783642460920. DOI: 10.1007/978-3-642-
354 46092-0. URL: <http://link.springer.com/10.1007/978-3-642-46092-0>.
- 355 [Ber71] Dimitri P. Bertsekas. “Control of Uncertain Systems with a Set-Membership Description
356 of Uncertainty”. PhD thesis. Cambridge, MA, USA: MIT, 1971.
- 357 [Pos75] E. Posner. “Random coding strategies for minimum entropy”. In: *IEEE Transactions on*
358 *Information Theory* 21.4 (July 1975), pp. 388–391. ISSN: 1557-9654. DOI: 10.1109/
359 TIT.1975.1055416.
- 360 [Rud91] Walter Rudin. *Functional analysis*. 2nd ed. International series in pure and applied
361 mathematics. New York: McGraw-Hill, 1991. 424 pp. ISBN: 9780070542365.
- 362 [McC97] Robert J. McCann. “A Convexity Principle for Interacting Gases”. In: *Advances in*
363 *Mathematics* 128.1 (June 1, 1997), pp. 153–179. ISSN: 0001-8708. DOI: 10.1006/aima.
364 1997.1634. URL: <https://www.sciencedirect.com/science/article/pii/S0001870897916340>.
- 366 [BB00] Jean-David Benamou and Yann Brenier. “A computational fluid mechanics solution
367 to the Monge-Kantorovich mass transfer problem”. In: *Numerische Mathematik* 84.3
368 (Jan. 1, 2000), pp. 375–393. ISSN: 0945-3245. DOI: 10.1007/s002110050002. URL:
369 <https://doi.org/10.1007/s002110050002>.
- 370 [DV00] Laurent Desvillettes and Cedric Villani. “On the spatially homogeneous landau equation
371 for hard potentials part i : existence, uniqueness and smoothness”. In: *Communica-*
372 *tions in Partial Differential Equations* 25.1 (Jan. 1, 2000), pp. 179–259. ISSN: 0360-
373 5302. DOI: 10.1080/03605300008821512. URL: [https://doi.org/10.1080/](https://doi.org/10.1080/03605300008821512)
374 [03605300008821512](https://doi.org/10.1080/03605300008821512).
- 375 [OV00] F. Otto and C. Villani. “Generalization of an Inequality by Talagrand and Links with
376 the Logarithmic Sobolev Inequality”. In: *Journal of Functional Analysis* 173.2 (June 1,
377 2000), pp. 361–400. ISSN: 0022-1236. DOI: 10.1006/jfan.1999.3557. URL: <https://www.sciencedirect.com/science/article/pii/S0022123699935577>.
- 379 [Gho02] B. K. Ghosh. “Probability Inequalities Related to Markov’s Theorem”. In: *The American*
380 *Statistician* 56.3 (2002), pp. 186–190. ISSN: 00031305. URL: <http://www.jstor.org/stable/3087296>.
- 382 [CMV03] José A. Carrillo, Robert J. McCann, and Cédric Villani. “Kinetic equilibration rates
383 for granular media and related equations: entropy dissipation and mass transporta-
384 tion estimates”. In: *Revista Matemática Iberoamericana* 19.3 (Dec. 2003), pp. 971–
385 1018. ISSN: 0213-2230. URL: [https://projecteuclid.org/journals/revista-](https://projecteuclid.org/journals/revista-matematica-iberoamericana/volume-19/issue-3/Kinetic-equilibration-rates-for-granular-media-and-related-equations/rmi/1077293812.full)
386 [matematica-iberoamericana/volume-19/issue-3/Kinetic-equilibration-](https://projecteuclid.org/journals/revista-matematica-iberoamericana/volume-19/issue-3/Kinetic-equilibration-rates-for-granular-media-and-related-equations/rmi/1077293812.full)
387 [rates-for-granular-media-and-related-equations/rmi/1077293812.](https://projecteuclid.org/journals/revista-matematica-iberoamericana/volume-19/issue-3/Kinetic-equilibration-rates-for-granular-media-and-related-equations/rmi/1077293812.full)
388 [full.](https://projecteuclid.org/journals/revista-matematica-iberoamericana/volume-19/issue-3/Kinetic-equilibration-rates-for-granular-media-and-related-equations/rmi/1077293812.full)
- 389 [Vil03a] Cédric Villani. *Topics in Optimal Transportation*. Vol. 58. Graduate Studies in
390 Mathematics. American Mathematical Society, Mar. 25, 2003. ISBN: 9780821833124
391 9780821872321 9781470418045. DOI: 10.1090/gsm/058. URL: <http://www.ams.org/gsm/058> (visited on 05/16/2023).
- 393 [Vil03b] Cédric Villani. *Topics in optimal transportation*. Vol. 58. Graduate Studies in Mathemat-
394 ics. American Mathematical Society, Providence, RI, 2003, pp. xvi+370. ISBN: 0-8218-
395 3312-X. DOI: 10.1090/gsm/058. URL: <https://doi.org/10.1090/gsm/058>.
- 396 [Ste04] J. Michael Steele. *The Cauchy-Schwarz Master Class: An Introduction to the Art of*
397 *Mathematical Inequalities*. Cambridge University Press, Apr. 26, 2004. 320 pp. ISBN:
398 9780521546775.
- 399 [AB06] “Correspondences”. In: *Infinite Dimensional Analysis: A Hitchhiker’s Guide*. Ed. by
400 Charalambos D. Aliprantis and Kim C. Border. Berlin, Heidelberg: Springer, 2006,
401 pp. 555–590. ISBN: 9783540295877. DOI: 10.1007/3-540-29587-9_17. URL:
402 https://doi.org/10.1007/3-540-29587-9_17.

- 403 [CMV06] José A. Carrillo, Robert J. McCann, and Cedric Villani. “Contractions in the 2-
404 Wasserstein Length Space and Thermalization of Granular Media”. In: *Archive for*
405 *Rational Mechanics and Analysis* 179.2 (Feb. 1, 2006), pp. 217–263. ISSN: 1432-0673.
406 DOI: 10.1007/s00205-005-0386-1. URL: [https://doi.org/10.1007/s00205-](https://doi.org/10.1007/s00205-005-0386-1)
407 [005-0386-1](https://doi.org/10.1007/s00205-005-0386-1) (visited on 05/24/2023).
- 408 [De106] Chrysanthos Dellarocas. “Strategic Manipulation of Internet Opinion Forums: Implica-
409 tions for Consumers and Firms”. In: *Management Science* 52.10 (Oct. 2006), pp. 1577–
410 1593. ISSN: 0025-1909, 1526-5501. DOI: 10.1287/mnsc.1060.0567. URL: <https://pubsonline.informs.org/doi/10.1287/mnsc.1060.0567> (visited on
411 [05/17/2023](https://pubsonline.informs.org/doi/10.1287/mnsc.1060.0567)).
- 413 [BCL09] Andrea L. Bertozzi, Jose A. Carrillo, and Thomas Laurent. “Blow-up in multidimensional
414 aggregation equations with mildly singular interaction kernels*”. In: *Nonlinearity* 22.3
415 (Feb. 2009), p. 683. ISSN: 0951-7715. DOI: 10.1088/0951-7715/22/3/009. URL:
416 <https://dx.doi.org/10.1088/0951-7715/22/3/009> (visited on 05/24/2023).
- 417 [BBS09] Steffen Bickel, Michael Brückner, and Tobias Scheffer. “Discriminative Learning Under
418 Covariate Shift”. In: *The Journal of Machine Learning Research* 10 (Dec. 1, 2009),
419 pp. 2137–2155. ISSN: 1532-4435.
- 420 [Bor09] Vivek S Borkar. *Stochastic approximation: a dynamical systems viewpoint*. Vol. 48.
421 Springer, 2009.
- 422 [DY10] Erick Delage and Yinyu Ye. “Distributionally Robust Optimization Under Moment
423 Uncertainty with Application to Data-Driven Problems”. In: *Operations Research* 58.3
424 (June 2010), pp. 595–612. ISSN: 0030-364X, 1526-5463. DOI: 10.1287/opre.1090.
425 0741. URL: [https://pubsonline.informs.org/doi/10.1287/opre.1090.](https://pubsonline.informs.org/doi/10.1287/opre.1090.0741)
426 [0741](https://pubsonline.informs.org/doi/10.1287/opre.1090.0741).
- 427 [LSW10] Juan Lang, Matt Spear, and S. Felix Wu. “Social Manipulation of Online Recommender
428 Systems”. In: *Social Informatics*. Ed. by Leonard Bolc, Marek Makowski, and Adam
429 Wierzbicki. Lecture Notes in Computer Science. Berlin, Heidelberg: Springer, 2010,
430 pp. 125–139. ISBN: 9783642165672. DOI: 10.1007/978-3-642-16567-2_10.
- 431 [CC11] Adriana Camacho and Emily Conover. “Manipulation of Social Program Eligibility”. In:
432 *American Economic Journal: Economic Policy* 3.2 (2011), pp. 41–65. ISSN: 1945-7731.
433 URL: <https://www.jstor.org/stable/41238093>.
- 434 [Car+11] J. A. Carrillo et al. “Global-in-time weak measure solutions and finite-time aggregation
435 for nonlocal interaction equations”. In: *Duke Mathematical Journal* 156.2 (Feb. 1,
436 2011). ISSN: 0012-7094. DOI: 10.1215/00127094-2010-211. URL: [https://projecteuclid.org/journals/duke-mathematical-journal/volume-156/](https://projecteuclid.org/journals/duke-mathematical-journal/volume-156/issue-2/Global-in-time-weak-measure-solutions-and-finite-time-aggregation/10.1215/00127094-2010-211.full)
437 [issue-2/Global-in-time-weak-measure-solutions-and-finite-time-](https://projecteuclid.org/journals/duke-mathematical-journal/volume-156/issue-2/Global-in-time-weak-measure-solutions-and-finite-time-aggregation/10.1215/00127094-2010-211.full)
438 [aggregation/10.1215/00127094-2010-211.full](https://projecteuclid.org/journals/duke-mathematical-journal/volume-156/issue-2/Global-in-time-weak-measure-solutions-and-finite-time-aggregation/10.1215/00127094-2010-211.full) (visited on 05/24/2023).
- 440 [BCY12] D. Balagu’e, J. Carrillo, and Y. Yao. “Confinement for repulsive-attractive ker-
441 nels”. In: *Discrete and Continuous Dynamical Systems-series B* (2012). URL:
442 [https://www.semanticscholar.org/paper/Confinement-](https://www.semanticscholar.org/paper/Confinement-for-repulsive-attractive-kernels-Balagu%27e-Carrillo/211b8c71330b956cd530ae9cc8aec03ff175b643)
443 [for-repulsive-attractive-kernels-Balagu%27e-Carrillo/](https://www.semanticscholar.org/paper/Confinement-for-repulsive-attractive-kernels-Balagu%27e-Carrillo/211b8c71330b956cd530ae9cc8aec03ff175b643)
444 [211b8c71330b956cd530ae9cc8aec03ff175b643](https://www.semanticscholar.org/paper/Confinement-for-repulsive-attractive-kernels-Balagu%27e-Carrillo/211b8c71330b956cd530ae9cc8aec03ff175b643) (visited on 05/24/2023).
- 445 [BLL12] Andrea L. Bertozzi, Thomas Laurent, and Flavien Lager. “Aggregation and spreading
446 via the newtonian potential: the dynamics of patch solutions”. In: *Mathematical Models*
447 *and Methods in Applied Sciences* 22 (supp01 Apr. 2012), p. 1140005. ISSN: 0218-2025.
448 DOI: 10.1142/S0218202511400057. URL: [https://www.worldscientific.com/](https://www.worldscientific.com/doi/abs/10.1142/S0218202511400057)
449 [doi/abs/10.1142/S0218202511400057](https://www.worldscientific.com/doi/abs/10.1142/S0218202511400057) (visited on 05/24/2023).
- 450 [FF13] Marco Di Francesco and Simone Fagioli. “Measure solutions for non-local interaction
451 PDEs with two species”. In: *Nonlinearity* 26.10 (Oct. 1, 2013), pp. 2777–2808. ISSN:
452 0951-7715, 1361-6544. DOI: 10.1088/0951-7715/26/10/2777. URL: <https://iopscience.iop.org/article/10.1088/0951-7715/26/10/2777>.
- 454 [PS13] Parag A. Pathak and Tayfun SÄ¶nmez. “School Admissions Reform in Chicago and
455 England: Comparing Mechanisms by Their Vulnerability to Manipulation”. In: *American*
456 *Economic Review* 103.1 (Feb. 2013), pp. 80–106. ISSN: 0002-8282. DOI: 10.1257/aer.
457 103.1.80. URL: [https://www.aeaweb.org/articles?id=10.1257/aer.103.1.](https://www.aeaweb.org/articles?id=10.1257/aer.103.1.80)
458 [80](https://www.aeaweb.org/articles?id=10.1257/aer.103.1.80) (visited on 05/16/2023).

- 459 [CCH14] José Antonio Carrillo, Michel Chipot, and Yanghong Huang. “On global minimizers
460 of repulsive-attractive power-law interaction energies”. In: *Philosophical Transactions
461 of the Royal Society A: Mathematical, Physical and Engineering Sciences* 372.2028
462 (Nov. 13, 2014), p. 20130399. ISSN: 1364-503X, 1471-2962. DOI: 10.1098/rsta.
463 2013.0399. URL: [https://royalsocietypublishing.org/doi/10.1098/rsta.
464 2013.0399](https://royalsocietypublishing.org/doi/10.1098/rsta.2013.0399) (visited on 05/24/2023).
- 465 [MKB14] Alan Mackey, Theodore Kolokolnikov, and Andrea L. Bertozzi. “Two-species particle
466 aggregation and stability of co-dimension one solutions”. In: *Discrete and Continuous
467 Dynamical Systems* 19.5 (2014), pp. 1411–1436.
- 468 [CCH15] José A. Carrillo, Alina Chertock, and Yanghong Huang. “A Finite-Volume Method
469 for Nonlinear Nonlocal Equations with a Gradient Flow Structure”. In: *Communications
470 in Computational Physics* 17.1 (Jan. 2015), pp. 233–258. ISSN: 1815-2406, 1991-
471 7120. DOI: 10.4208/cicp.160214.010814a. URL: [https://www.cambridge.
472 org/core/journals/communications-in-computational-physics/article/
473 abs/finitevolume-method-for-nonlinear-nonlocal-equations-with-a-
474 gradient-flow-structure/018EF83B9419424E1A34DB9492288FA4](https://www.cambridge.org/core/journals/communications-in-computational-physics/article/abs/finitevolume-method-for-nonlinear-nonlocal-equations-with-a-gradient-flow-structure/018EF83B9419424E1A34DB9492288FA4).
- 475 [Per15] Benoît Perthame. *Parabolic Equations in Biology: Growth, reaction, movement and
476 diffusion*. Lecture Notes on Mathematical Modelling in the Life Sciences. Cham: Springer
477 International Publishing, 2015. ISBN: 9783319194998 9783319195001. DOI: 10.1007/
478 978-3-319-19500-1. URL: [https://link.springer.com/10.1007/978-3-319-
479 19500-1](https://link.springer.com/10.1007/978-3-319-19500-1) (visited on 05/24/2023).
- 480 [San15a] Filippo Santambrogio. *Optimal Transport for Applied Mathematicians*. 2015. URL:
481 <http://math.univ-lyon1.fr/~santambrogio/OTAM-cvgmt.pdf>.
- 482 [San15b] Filippo Santambrogio. “Optimal Transport for Applied Mathematicians. Calculus of
483 Variations, PDEs and Modeling”. In: (2015). URL: [https://www.math.u-psud.fr/
484 ~filippo/OTAM-cvgmt.pdf](https://www.math.u-psud.fr/~filippo/OTAM-cvgmt.pdf).
- 485 [Har+16] Moritz Hardt et al. “Strategic Classification”. In: *Proceedings of the 2016 ACM
486 Conference on Innovations in Theoretical Computer Science*. ITCS ’16. New York,
487 NY, USA: Association for Computing Machinery, Jan. 14, 2016, pp. 111–122. ISBN:
488 9781450340571. DOI: 10.1145/2840728.2840730. URL: [https://doi.org/10.
489 1145/2840728.2840730](https://doi.org/10.1145/2840728.2840730).
- 490 [Bur+18] Martin Burger et al. “Sorting Phenomena in a Mathematical Model For Two Mutually
491 Attracting/Repelling Species”. In: *SIAM Journal on Mathematical Analysis* 50.3 (Jan. 1,
492 2018), pp. 3210–3250. ISSN: 0036-1410. DOI: 10.1137/17M1125716. URL: [https:
493 //doi.org/10.1137/17M1125716](https://doi.org/10.1137/17M1125716).
- 494 [CHS18] José A. Carrillo, Yanghong Huang, and Markus Schmidtchen. “Zoology of a Nonlocal
495 Cross-Diffusion Model for Two Species”. In: *SIAM Journal on Applied Mathematics* 78.2
496 (Jan. 2018), pp. 1078–1104. ISSN: 0036-1399, 1095-712X. DOI: 10.1137/17M1128782.
497 URL: <https://epubs.siam.org/doi/10.1137/17M1128782>.
- 498 [Don+18] Jinshuo Dong et al. “Strategic classification from revealed preferences”. In: *Proceedings
499 of the 2018 ACM Conference on Economics and Computation*. 2018, pp. 55–70.
- 500 [Ree18] Alex Rees-Jones. “Suboptimal behavior in strategy-proof mechanisms: Evidence from the
501 residency match”. In: *Games and Economic Behavior*. Special Issue in Honor of Lloyd
502 Shapley: Seven Topics in Game Theory 108 (Mar. 1, 2018), pp. 317–330. ISSN: 0899-
503 8256. DOI: 10.1016/j.geb.2017.04.011. URL: [https://www.sciencedirect.
504 com/science/article/pii/S0899825617300751](https://www.sciencedirect.com/science/article/pii/S0899825617300751) (visited on 05/16/2023).
- 505 [Kuh+19] Daniel Kuhn et al. “Wasserstein Distributionally Robust Optimization: Theory and
506 Applications in Machine Learning”. In: *Operations Research & Management Science in
507 the Age of Analytics*. Ed. by Serguei Netessine, Douglas Shier, and Harvey J. Greenberg.
508 INFORMS, Oct. 2019, pp. 130–166. ISBN: 9780990615330. DOI: 10.1287/educ.2019.
509 0198. URL: <http://pubsonline.informs.org/doi/10.1287/educ.2019.0198>.
- 510 [DS20] Tomasz Debiec and Markus Schmidtchen. “Incompressible Limit for a Two-Species
511 Tumour Model with Coupling Through Brinkman’s Law in One Dimension”. In: *Acta
512 Applicandae Mathematicae* 169.1 (Oct. 1, 2020), pp. 593–611. ISSN: 1572-9036. DOI:
513 10.1007/s10440-020-00313-1. URL: [https://doi.org/10.1007/s10440-020-
514 00313-1](https://doi.org/10.1007/s10440-020-00313-1).

- 515 [DT20] Manh Hong Duong and Julian Tugaut. “Coupled McKean-Vlasov diffusions: wellposed-
516 ness, propagation of chaos and invariant measures”. In: *Stochastics* 92.6 (Aug. 17, 2020),
517 pp. 900–943. ISSN: 1744-2508. DOI: 10 . 1080 / 17442508 . 2019 . 1677663. URL:
518 <https://doi.org/10.1080/17442508.2019.1677663>.
- 519 [FCR20] Tanner Fiez, Benjamin Chasnov, and Lillian Ratliff. “Implicit learning dynamics in
520 stackelberg games: Equilibria characterization, convergence analysis, and empirical
521 study”. In: *International Conference on Machine Learning*. PMLR. 2020, pp. 3133–
522 3144.
- 523 [Mil+20] John Miller et al. “The Effect of Natural Distribution Shift on Question Answering
524 Models”. In: *Proceedings of the 37th International Conference on Machine Learning*.
525 International Conference on Machine Learning. PMLR, Nov. 21, 2020, pp. 6905–6916.
526 URL: <https://proceedings.mlr.press/v119/miller20a.html>.
- 527 [Per+20] Juan Perdomo et al. “Performative Prediction”. In: *Proceedings of the 37th Interna-*
528 *tional Conference on Machine Learning*. International Conference on Machine Learning.
529 PMLR, Nov. 21, 2020, pp. 7599–7609. URL: <https://proceedings.mlr.press/v119/perdomo20a.html>.
- 531 [AB21] Abdulaziz Alsenafi and Alethea B. T. Barbaro. “A Multispecies Cross-Diffusion Model
532 for Territorial Development”. In: *Mathematics* 9.12 (Jan. 2021), p. 1428. ISSN: 2227-
533 7390. DOI: 10.3390/math9121428. URL: [https://www.mdpi.com/2227-7390/9/
534 12/1428](https://www.mdpi.com/2227-7390/9/12/1428).
- 535 [DN21] John C. Duchi and Hongseok Namkoong. “Learning models with uniform perfor-
536 mance via distributionally robust optimization”. In: *The Annals of Statistics* 49.3 (June
537 2021), pp. 1378–1406. ISSN: 0090-5364, 2168-8966. DOI: 10 . 1214 / 20 - AOS2004.
538 URL: [https://projecteuclid.org/journals/annals-of-statistics/
539 volume-49/issue-3/Learning-models-with-uniform-performance-via-
540 distributionally-robust-optimization/10.1214/20-AOS2004.full](https://projecteuclid.org/journals/annals-of-statistics/volume-49/issue-3/Learning-models-with-uniform-performance-via-distributionally-robust-optimization/10.1214/20-AOS2004.full).
- 541 [FR21] Tanner Fiez and Lillian J Ratliff. “Local convergence analysis of gradient descent ascent
542 with finite timescale separation”. In: *Proceedings of the International Conference on
543 Learning Representation*. 2021.
- 544 [Fie+21] Tanner Fiez et al. “Global convergence to local minmax equilibrium in classes of non-
545 convex zero-sum games”. In: *Advances in Neural Information Processing Systems* 34
546 (2021), pp. 29049–29063.
- 547 [IYZ21] Zachary Izzo, Lexing Ying, and James Zou. “How to Learn when Data Reacts to Your
548 Model: Performative Gradient Descent”. In: *Proceedings of the 38th International Con-*
549 *ference on Machine Learning*. International Conference on Machine Learning. PMLR,
550 July 1, 2021, pp. 4641–4650. URL: [https://proceedings.mlr.press/v139/
551 izzo21a.html](https://proceedings.mlr.press/v139/izzo21a.html).
- 552 [LHL21] Qi Lei, Wei Hu, and Jason D. Lee. “Near-Optimal Linear Regression under Distribution
553 Shift”. In: *ArXiv* (June 23, 2021). URL: [https://www.semanticscholar.org/
554 paper/Near-Optimal-Linear-Regression-under-Distribution-Lei-Hu/
555 8d58212f38852aba3eccb8f3900299a495bba8e0](https://www.semanticscholar.org/paper/Near-Optimal-Linear-Regression-under-Distribution-Lei-Hu/8d58212f38852aba3eccb8f3900299a495bba8e0).
- 556 [Liu+21] Lewis Liu et al. “Infinite-Dimensional Optimization for Zero-Sum Games via Variational
557 Transport”. In: *Proceedings of the 38th International Conference on Machine Learning*.
558 International Conference on Machine Learning. PMLR, July 1, 2021, pp. 7033–7044.
559 URL: <https://proceedings.mlr.press/v139/liu21ac.html>.
- 560 [MPZ21] John P Miller, Juan C Perdomo, and Tijana Zrnic. “Outside the echo chamber: Optimizing
561 the performative risk”. In: *International Conference on Machine Learning*. PMLR. 2021,
562 pp. 7710–7720.
- 563 [Wil+21] Olivia Wiles et al. “A Fine-Grained Analysis on Distribution Shift”. In: *ArXiv*
564 (Oct. 21, 2021). URL: [https://www.semanticscholar.org/paper/A-
565 Fine-Grained-Analysis-on-Distribution-Shift-Wiles-Gowal/
566 0e845ef0a3ae71bd32a6954fafa0702d0f0f033f](https://www.semanticscholar.org/paper/A-Fine-Grained-Analysis-on-Distribution-Shift-Wiles-Gowal/0e845ef0a3ae71bd32a6954fafa0702d0f0f033f).
- 567 [Zrn+21] Tijana Zrnic et al. “Who Leads and Who Follows in Strategic Classification?” In: *Ad-*
568 *vances in Neural Information Processing Systems*. Vol. 34. Curran Associates, Inc., 2021,
569 pp. 15257–15269. URL: [https://proceedings.neurips.cc/paper/2021/hash/
570 812214fb8e7066bfa6e32c626c2c688b-Abstract.html](https://proceedings.neurips.cc/paper/2021/hash/812214fb8e7066bfa6e32c626c2c688b-Abstract.html).

- 571 [AZ22] Alekh Agarwal and Tong Zhang. “Minimax Regret Optimization for Robust Machine
572 Learning under Distribution Shift”. In: *Proceedings of Thirty Fifth Conference on Learn-
573 ing Theory*. Conference on Learning Theory. PMLR, June 28, 2022, pp. 2704–2729.
574 URL: <https://proceedings.mlr.press/v178/agarwal22b.html>.
- 575 [Giu+22] Valeria Giunta et al. “Local and Global Existence for Nonlocal Multispecies Advection-
576 Diffusion Models”. In: *SIAM Journal on Applied Dynamical Systems* 21.3 (Sept. 2022),
577 pp. 1686–1708. ISSN: 1536-0040. DOI: 10.1137/21M1425992. URL: <https://epubs.siam.org/doi/10.1137/21M1425992>.
- 579 [JPZ22] Ansgar Jungel, Stefan Portisch, and Antoine Zurek. “Nonlocal cross-diffusion systems
580 for multi-species populations and networks”. In: *Nonlinear Analysis* 219 (June 1, 2022),
581 p. 112800. ISSN: 0362-546X. DOI: 10.1016/j.na.2022.112800. URL: <https://www.sciencedirect.com/science/article/pii/S0362546X22000153>.
- 583 [LY22] Guanlin Li and Yao Yao. “Two-species competition model with chemotaxis: well-
584 posedness, stability and dynamics”. In: *Nonlinearity* 35.3 (Feb. 3, 2022), p. 1329. ISSN:
585 0951-7715. DOI: 10.1088/1361-6544/ac4a8d. URL: <https://iopscience.iop.org/article/10.1088/1361-6544/ac4a8d/meta>.
- 587 [LFG22] Fengming Lin, Xiaolei Fang, and Zheming Gao. “Distributionally Robust Optimization:
588 A review on theory and applications”. In: *Numerical Algebra, Control and Optimization*
589 12.1 (2022), pp. 159–212.
- 590 [Nar+22] Adhyayan Narang et al. “Learning in Stochastic Monotone Games with Decision-
591 Dependent Data”. In: *International Conference on Artificial Intelligence and Statistics*.
592 PMLR, 2022, pp. 5891–5912.
- 593 [Ray+22] Mitas Ray et al. “Decision-dependent risk minimization in geometrically decaying dy-
594 namic environments”. In: *Proceedings of the AAAI Conference on Artificial Intelligence*.
595 Vol. 36. 7. 2022, pp. 8081–8088.
- 596 [CFG23] J. Carrillo, Alejandro Fernandez-Jimenez, and D. Gómez-Castro. “Partial mass concen-
597 tration for fast-diffusions with non-local aggregation terms”. In: Apr. 10, 2023. URL:
598 [https://www.semanticscholar.org/paper/Partial-mass-concentration-
599 for-fast-diffusions-with-Carrillo-Fern%C3%A1ndez-Jim%C3%A9nez/
600 5d1a0923f6bdaf24337c8161d6119175c406de5a](https://www.semanticscholar.org/paper/Partial-mass-concentration-for-fast-diffusions-with-Carrillo-Fern%C3%A1ndez-Jim%C3%A9nez/5d1a0923f6bdaf24337c8161d6119175c406de5a) (visited on 05/24/2023).
- 601 [Qui+] Joaquin Quinero-Candela et al. *Dataset Shift in Machine Learning*. MIT Press. URL:
602 [https://mitpress.mit.edu/9780262545877/dataset-shift-in-machine-
603 learning/](https://mitpress.mit.edu/9780262545877/dataset-shift-in-machine-learning/).

604 A General structure and preliminaries

605 In this section, we give more details on the models discussed in the main article, and introduce definitions and
606 notation that are needed for the subsequent proofs.

607 A.1 Structure of the dynamics

608 For the case of aligned objectives, the full coupled system of PDEs (3) can be written as

$$\partial_t \rho = \alpha \Delta \rho + \operatorname{div} \left(\rho \nabla_z \left(\int f_1 d\mu - \alpha \log \tilde{\rho} + W * \rho \right) \right), \quad (6a)$$

$$\partial_t \mu = \operatorname{div} \left(\mu \nabla_x \left(\int f_1 d\rho + \int f_2 d\bar{\rho} + \frac{\beta}{2} \|x - x_0\|^2 \right) \right). \quad (6b)$$

609 In other words, the population ρ in (6a) is subject to an isotropic diffusive force with diffusion coefficient $\alpha > 0$,
610 a drift force driven by the time-varying confining potential $\int f_1 d\mu(t) - \alpha \log \tilde{\rho}$, and a self-interaction force via
611 the interaction potential W . If we consider the measure μ to be given and fixed in time, this corresponds exactly
612 to the type of parabolic equation studied in [CMV03]. Here however the dynamics are more complex due to
613 the coupling of the confining potential with the dynamics (6b) for $\mu(t)$ via the coupling potential f_1 . Before
614 presenting the analysis of this model, let us give a bit more intuition on the meaning and the structure of these
615 dynamics.

616 In the setting where μ represents a binary classifier, we can think of the distribution $\bar{\rho}$ as all those individuals
617 carrying the true label 1, say, and the distribution $\rho(t)$ as all those individuals carrying a true label 0, say. The
618 term $\int f_1(z, x) \mu(t, dx)$ represents a penalty for incorrectly classifying an individual at z with true label 0
619 when using the classifier $\mu(t, x)$. In other words, $\int f_1(z, x) \mu(t, dx) \in [0, \infty)$ is increasingly large the more
620 z digresses from the correct classification 0. Similarly, $\int f_1(z, x) \rho(t, dz) \in [0, \infty)$ is increasingly large if
621 the population ρ shifts mass to locations in z where the classification is incorrect. The terminology *aligned*
622 *objectives* refers to the fact that in (6) both the population and the classifier are trying to evolve in a way as to
623 maximize correct classification. Analogously, the term $\int f_2(z, x) \bar{\rho}(dz)$ is large if x would incorrectly classify
624 the population $\bar{\rho}$ that carries the label 1. A natural extension of the model (6) would be a setting where also the
625 population carrying labels 1 evolves over time, which is simulated in Section E.2. Most elements of the new
626 framework presented here would likely carry over the setting of three coupled PDEs: one for the evolution of
627 $\rho(t)$, one for the evolution of $\bar{\rho}(t)$ and one for the classifier $\mu(t)$.

The term

$$\alpha \Delta \rho - \alpha \operatorname{div} (\rho \nabla \log \tilde{\rho}) = \alpha \operatorname{div} (\rho \nabla \delta_\rho KL(\rho | \tilde{\rho}))$$

628 forces the evolution of $\rho(t)$ to approach $\tilde{\rho}$. In other words, it penalizes (in energy) deviations from a given
629 reference measure $\tilde{\rho}$. In the context of the application at hand, we take $\tilde{\rho}$ to be the initial distribution $\rho(t=0)$.
630 The solution $\rho(t)$ then evolves away from $\tilde{\rho}$ over time due to the other forces that are present. Therefore, the
631 term $KL(\rho | \tilde{\rho})$ in the energy both provides smoothing of the flow and a penalization for deviations away from
632 the reference measure $\tilde{\rho}$.

The self-interaction term $W * \rho$ introduces non-locality into the dynamics, as the decision for any given individual
to move in a certain direction is influenced by the behavior of all other individuals in the population. The choice
of W is application dependent. Very often, the interaction between two individuals only depends on the distance
between them. This suggests a choice of W as a radial function, i.e. $W(z) = \omega(|z|)$. A choice of $\omega : \mathbb{R} \rightarrow \mathbb{R}$
such that $\omega'(r) > 0$ corresponds to an *attractive* force between individuals, whereas $\omega'(r) < 0$ corresponds to a
repulsive force. The statement $|z| \omega'(|z|) = z \cdot \nabla_z W(z) \geq -D$ in Assumption 3 therefore corresponds to a
requirement that the self-interaction force is not too repulsive. Neglecting all other forces in (6a), we obtain the
non-local interaction equation

$$\partial_t \rho = \operatorname{div} (\rho \nabla W * \rho)$$

633 which appears in many instances in mathematical biology, mathematical physics, and material science, and it
634 is an equation that has been extensively studied over the past few decades, see for example [Car+11; BCY12;
635 CCH14; BCL09; BLL12; CMV06; CFG23] and references therein. Using the results from these works, our
636 assumptions on the interaction potential W can be relaxed in many ways, for example by allowing discontinuous
637 derivatives at zero for W , or by allowing W to be negative.

The dynamics (6b) for the algorithm μ is a non-autonomous transport equation,

$$\partial_t \mu = \operatorname{div} (\mu v),$$

where the time-dependence in the velocity field

$$v(t, x) := \nabla_x \left(\int f_1(z, x) d\rho(t, z) + \int f_2(z, x) d\bar{\rho}(z) + \frac{\beta}{2} \|x - x_0\|^2 \right),$$

638 comes through the evolving population $\rho(t)$. This structure allows to obtain an explicit solution for $\mu(t)$ in
639 terms of the initial condition μ_0 and the solution $\rho(t)$ to (6a) using the methods of characteristics.

640 **Proposition 4.** Assume that f_1 and f_2 are Lipschitz in x uniformly in z . Then the unique distributional solution
641 $\mu(t)$ to (6b) is given by

$$\mu(t) = \Phi(t, 0, \cdot) \# \mu_0, \quad (7)$$

642 where $\Phi(t, s, x)$ solves the characteristic equation

$$\partial_s \Phi(s, t, x) + v(s, \Phi(s, t, x)) = 0, \quad \Phi(t, t, x) = x. \quad (8)$$

643 *Proof.* Thanks to Assumption 1, we have that $v \in C^1(\mathbb{R} \times \mathbb{R}^d; \mathbb{R}^d)$. Moreover, we claim that the velocity field
644 v satisfies

$$\|v(t, x)\| \leq c(1 + \|x\|) \quad \text{for all } t \geq 0, x \in \mathbb{R}^d \quad (9)$$

645 for some constant $c > 0$ independent of t and x . By classical Cauchy-Lipschitz theory for ODEs, this guarantees
646 the existence of a unique global solution $\Phi(t, s, x)$ solving (8). Then it can be checked directly that $\mu(t)$ as
647 defined in (7) is a distributional solution to (6b).

648 It remains to prove the bound (9). Thanks to the Lipschitz assumption together with Assumption 1, we have that
649 $\|\nabla_x f_1(z, x) + \nabla_x f_2(z, x)\| \leq c$ for all $z, x \in \mathbb{R}^d$ for some constant $c > 0$. Therefore, we have

$$\left\| \int \nabla_x f_1(z, x) d\rho(z) + \int \nabla_x f_2(z, x) d\bar{\rho}(z) + \beta(x - x_0) \right\| \leq c'(1 + \|x\|)$$

650 for another constant $c' > 0$. □

651 **Remark 2.** The Lipschitz assumption on f_1 and f_2 can be relaxed as long as we can still guarantee that (9)
652 holds.

653 In the characteristic equation (8), $\Phi(s, t, x)$ is a parametrization of all trajectories: if a particle was at location
654 x at time t , then it is at location $\Phi(s, t, x)$ at time s . Our assumptions on f_1, f_2 and $\bar{\rho}$ also ensure that
655 $\Phi(s, t, \cdot) : \mathbb{R}^d \rightarrow \mathbb{R}^d$ is a C^1 -diffeomorphism for all $s, t \in \mathbb{R}$. For more details on transport equations, see for
656 example [Per15, Chapter 8.4].

657 **Remark 3.** Consider the special case where $\mu_0 = \delta_{x_0}$ for some initial position $x_0 \in \mathbb{R}^d$. Then by Proposition 4,
658 the solution to (6b) is given by $\mu(t) = \delta_{x(t)}$, where $x(t) := \Phi(t, 0, x_0)$ solves the ODE

$$\dot{x}(t) = -v(t, x(t)), \quad x(0) = x_0,$$

659 which is precisely of type (2).

660 For the case of competing objectives, the two models we consider can be written as

$$\begin{aligned} \partial_t \rho &= -\operatorname{div}(\rho(\nabla(f_1(z, b(\rho)) - \alpha \log(\rho/\bar{\rho}) - \rho W * \rho)), \\ b(\rho) &:= \operatorname{argmin}_{\bar{x}} \int f_1(z, \bar{x}) d\rho(z) + \int f_2(\bar{x}, z') d\bar{\rho}(z') + \frac{\beta}{2} \|\bar{x} - x_0\|^2 \end{aligned}$$

661 for (4), and

$$\begin{aligned} \frac{d}{dt} x &= -\nabla_x \left(\int f_1(z, x) r(x) (dz) + \int f_2(x, z') d\bar{\rho}(z') + \frac{\beta}{2} \|x - x_0\|^2 \right), \\ r(x) &:= \operatorname{argmax}_{\hat{\rho} \in \mathcal{P}} \int f_1(z, x) d\hat{\rho}(z) - \alpha KL(\hat{\rho}|\bar{\rho}) - \frac{1}{2} \int \hat{\rho} W * \hat{\rho}. \end{aligned}$$

662 for (5).

663 A.2 Definitions and notation

Here, and in what follows, I_d denotes the $d \times d$ identity matrix, and id denotes the identity map. The energy functionals we are considering are usually defined on the set of probability measures on \mathbb{R}^d , denoted by $\mathcal{P}(\mathbb{R}^d)$. If we consider the subset $\mathcal{P}_2(\mathbb{R}^d)$ of probability measures with bounded second moment,

$$\mathcal{P}_2(\mathbb{R}^d) := \{\rho \in \mathcal{P}(\mathbb{R}^d) : \int_{\mathbb{R}^d} \|z\|^2 d\rho(z) < \infty\},$$

664 then we can endow this space with the Wasserstein-2 metric.

665 **Definition 3** (Wasserstein Metric). The Wasserstein metric between two probability measures $\mu, \nu \in \mathcal{P}_2(\mathbb{R}^d)$ is
666 given by

$$W_2(\mu, \nu)^2 = \inf_{\gamma \in \Gamma(\mu, \nu)} \int \|z - z'\|_2^2 d\gamma(z, z')$$

667 where Γ is the set of all joint probability distributions with marginals μ and ν , i.e. $\mu(dz) = \int \gamma(dz, z') dz'$ and
668 $\nu(dz') = \int \gamma(z, dz') dz$.

669 The restriction to $\mathcal{P}_2(\mathbb{R}^d)$ ensures that the W_2 is always finite. Then the space $(\mathcal{P}_2(\mathbb{R}^d), W_2)$ is indeed a metric
670 space. We will make use of the fact that W_2 metrizes narrow convergence of probability measures. To make this
671 statement precise, let us introduce two common notions of convergence for probability measures, which are a
672 subset of the finite signed Radon measures $\mathcal{M}(\mathbb{R}^d)$.

673 **Definition 4.** Consider a sequence $(\mu_n) \in \mathcal{M}(\mathbb{R}^d)$ and a limit $\mu \in \mathcal{M}(\mathbb{R}^d)$.

- **(Narrow topology)** The sequence (μ_n) converges narrowly to μ , denoted by $\mu_n \rightarrow \mu$, if for all continuous bounded functions $f : \mathbb{R}^d \rightarrow \mathbb{R}$,

$$\int_{\mathbb{R}^d} f(z) d\mu_n(z) \rightarrow \int_{\mathbb{R}^d} f(z) d\mu(z).$$

- **(Weak-* topology)** The sequence (μ_n) converges weakly-* to μ , denoted by $\mu_n \xrightarrow{*} \mu$, if for all continuous functions vanishing at infinity (i.e. $f : \mathbb{R}^d \rightarrow \mathbb{R}$ such that for all $\epsilon > 0$ there exists a compact set $K \subset \mathbb{R}^d$ such that $|f(z)| < \epsilon$ on $\mathbb{R}^d \setminus K$), we have

$$\int_{\mathbb{R}^d} f(z) d\mu_n(z) \rightarrow \int_{\mathbb{R}^d} f(z) d\mu(z).$$

674 Let us denote the set of continuous functions on \mathbb{R}^d vanishing at infinity by $C_0(\mathbb{R}^d)$, and the set of continuous
675 bounded functions by $C_b(\mathbb{R}^d)$. Note that narrow convergence immediately implies that $\mu_n(\mathbb{R}^d) \rightarrow \mu(\mathbb{R}^d)$ as
676 the constant function is in $C_b(\mathbb{R}^d)$. This is not necessarily true for weak-* convergence. We will later make use
677 of the Banach-Alaoglu theorem [Ala40], which gives weak-* compactness of the unit ball in a dual space. Note
678 that $\mathcal{M}(\mathbb{R}^d)$ is indeed the dual of $C_0(\mathbb{R}^d)$, and $\mathcal{P}(\mathbb{R}^d)$ is the unit ball in $\mathcal{M}(\mathbb{R}^d)$ using the dual norm. Moreover,
679 if we can ensure that mass does not escape to infinity, the two notions of convergence in Definition 4 are in fact
680 equivalent.

681 **Lemma 5.** Consider a sequence $(\mu_n) \in \mathcal{M}(\mathbb{R}^d)$ and a measure $\mu \in \mathcal{M}(\mathbb{R}^d)$. Then $\mu_n \rightarrow \mu$ if and only if
682 $\mu_n \xrightarrow{*} \mu$ and $\mu_n(\mathbb{R}^d) \rightarrow \mu(\mathbb{R}^d)$.

683 This follows directly from Definition 4. Here, the condition $\mu_n(\mathbb{R}^d) \rightarrow \mu(\mathbb{R}^d)$ is equivalent to tightness of (μ_n) ,
684 and follows from Markov's inequality [Gho02] if we can establish uniform bounds on the second moments, i.e.
685 we want to show that there exists a constant $C > 0$ independent of n such that

$$\int \|x\|^2 d\mu_n(x) < C \quad \forall n \in \mathbb{N}. \quad (10)$$

686

687 **Definition 5** (Tightness of probability measures). A collection of measures $(\mu_n) \in \mathcal{M}(\mathbb{R}^d)$ is tight if for all
688 $\epsilon > 0$ there exists a compact set $K_\epsilon \subset \mathbb{R}^d$ such that $|\mu_n|(\mathbb{R}^d \setminus K_\epsilon) < \epsilon$ for all $n \in \mathbb{N}$, where $|\mu|$ denotes the
689 total variation of μ .

690 Another classical result is that the Wasserstein-2 metric metrizes narrow convergence of probability measures,
691 see for example [San15a, Theorem 5.11] or [Vil03a, Theorem 7.12].

692 **Lemma 6.** Let $\mu_n, \mu \in \mathcal{P}_2(\mathbb{R}^d)$. Then $W_2(\mu_n, \mu) \rightarrow 0$ if and only if

$$\mu_n \xrightarrow{*} \mu \quad \text{and} \quad \int_{\mathbb{R}^d} \|z\|^2 d\mu_n(z) \rightarrow \int_{\mathbb{R}^d} \|z\|^2 d\mu(z).$$

693 Next, we consider two measures $\mu, \nu \in \mathcal{P}(\mathbb{R}^d)$ that are atomless, i.e. $\mu(\{z\}) = 0$ for all $z \in \mathbb{R}^d$. By Brenier's
694 theorem [BB00] (also see [Vil03a, Theorem 2.32]) there exists a unique measurable map $T : \mathbb{R}^d \rightarrow \mathbb{R}^d$ such
695 that $T_{\#}\mu = \nu$, and $T = \nabla\psi$ for some convex function $\psi : \mathbb{R}^d \rightarrow \mathbb{R}$. Here, the push-forward operator $\nabla\psi_{\#}$ is
696 defined as

$$\int_{\mathbb{R}^d} f(z) d\nabla\psi_{\#}\rho_0(z) = \int_{\mathbb{R}^d} f(\nabla\psi(z)) d\rho_0(z)$$

697 for all Borel-measurable functions $f : \mathbb{R}^d \rightarrow \mathbb{R}_+$. If $\rho_1 = \nabla\psi_{\#}\rho_0$, we denote by $\rho_t = [(1-t)\text{id} + t\nabla\psi]_{\#}\rho_0$
698 the displacement interpolant between ρ_0 and ρ_1 . We are now ready to introduce the notion of displacement
699 convexity, which is the same as geodesic convexity in the geodesic space $(\mathcal{P}_2(\mathbb{R}^d), W_2)$. We will state the
700 definition here for atomless measures, but it can be relaxed to any measures in \mathcal{P}_2 using optimal transport plans
701 instead of transport maps.

702 **Definition 6** (Displacement Convexity). A functional $G : \mathcal{P} \rightarrow \mathbb{R}$ is displacement convex if for all ρ_0, ρ_1 that
703 are atomless we have

$$G(\rho_t) \leq (1-t)G(\rho_0) + tG(\rho_1),$$

704 where $\rho_t = [(1-t)\text{id} + t\nabla\psi]_{\#}\rho_0$ is the displacement interpolant between ρ_0 and ρ_1 . Further, $G : \mathcal{P} \mapsto \mathbb{R}$ is
 705 uniformly displacement convex with constant $\eta > 0$ if

$$G(\rho_t) \leq (1-t)G(\rho_0) + tG(\rho_1) - t(1-t)\frac{\eta}{2}W_2(\rho_0, \rho_1)^2,$$

706 where $\rho_t = [(1-t)\text{id} + t\nabla\psi]_{\#}\rho_0$ is the displacement interpolant between ρ_0 and ρ_1 .

707 **Remark 4.** In other words, G is displacement convex (concave) if the function $G(\rho_t)$ is convex (concave) with
 708 $\rho_t = [(1-t)\text{id} + t\nabla\psi]_{\#}\rho_0$ being the displacement interpolant between ρ_0 and ρ_1 . Contrast this with the
 709 classical notion of convexity (concavity) for G , where we require that the function $G((1-t)\rho_0 + t\rho_1)$ is convex
 710 (concave).

711 In fact, if the energy G is twice differentiable along geodesics, then the condition $\frac{d^2}{ds^2}G(\gamma_s) \geq 0$ along
 712 any geodesic $(\rho_s)_{s \in [0,1]}$ between ρ_0 and ρ_1 is sufficient to obtain displacement convexity. Similarly, when
 713 $\frac{d^2}{ds^2}G(\rho_s) \geq \eta W_2(\rho_0, \rho_1)^2$, then G is uniformly displacement convex with constant $\eta > 0$. For more details,
 714 see [McC97] and [Vil03a, Chapter 5.2].

715 Finally, we introduce a notion of derivative in infinite dimensions. This expression appears when computing the
 716 gradient of an energy in the Wasserstein-2 topology.

717 **Definition 7** (First Variation). For a map $G : \mathcal{P}(\mathbb{R}^d) \mapsto \mathbb{R}$ and fixed probability distribution $\rho \in \mathcal{P}(\mathbb{R}^d)$, the
 718 first variation of G at the point ρ is denoted by $\delta_\rho G[\rho] : \mathbb{R}^d \rightarrow \mathbb{R}$, and is defined via the relation

$$\int \delta_\rho G[\rho](z)\psi(z)dz = \lim_{\epsilon \rightarrow 0} \frac{1}{\epsilon}(G(\rho + \epsilon\psi) - G(\rho))$$

719 for all ψ such that $\int d\psi = 0$, assuming that G is regular enough for all quantities to exist.

720 Using the first variation, we can express the gradient in Wasserstein-2 space, see for example [Vil03a, Exercise
 721 8.8].

Lemma 7. The gradient of an energy $G : \mathcal{P}_2(\mathbb{R}^d) \rightarrow \mathbb{R}$ in the Wasserstein-2 space is given by

$$\nabla_{W_1} G(\rho) = -\text{div}(\rho \nabla \delta_\rho G[\rho]).$$

722 As a consequence, the infinite dimensional steepest descent in Wasserstein-2 space can be expressed as the PDE

$$\partial_t \rho = -\nabla_{W_1} G(\rho) = \text{div}(\rho \nabla \delta_\rho G[\rho]). \quad (11)$$

723 All the coupled gradient flows considered in this work have this Wasserstein-2 structure.

724 A.3 Steady states

725 The main goal in our theoretical analysis is to characterize the asymptotic behavior for the models (3), (4) and
 726 (5) as time goes to infinity. The steady states of these equations are the natural candidates to be asymptotic
 727 profiles for the corresponding equations. Thanks to the gradient flow structure, we expect to be able to make a
 728 connection between ground states of the energy functionals, and the steady state of the corresponding gradient
 729 flow dynamics. More precisely, any minimizer or maximizer is in particular a critical point of the energy, and
 730 therefore satisfies that the first variation is constant on disconnected components of the support. If this ground
 731 state also has enough regularity (weak differentiability) to be a solution to the equation, it immediately follows
 732 that it is in fact a steady state.

733 To make this connection precise, we first introduce what exactly we mean by a steady state.

734 **Definition 8** (Steady states for (3)). Given $\rho_\infty \in L^1_+(\mathbb{R}^d) \cap L^\infty_{loc}(\mathbb{R}^d)$ with $\|\rho_\infty\|_1 = 1$ and $\mu_\infty \in \mathcal{P}_2(\mathbb{R}^d)$,
 735 then $(\rho_\infty, \mu_\infty)$ is a steady state for the system (3) if $\rho_\infty \in W^{1,2}_{loc}(\mathbb{R}^d)$, $\nabla W * \rho_\infty \in L^1_{loc}(\mathbb{R}^d)$, ρ_∞ is absolutely
 736 continuous with respect to $\tilde{\rho}$, and $(\rho_\infty, \mu_\infty)$ satisfy

$$\nabla_z \left(\int f_1(z, x) d\mu_\infty(x) + \alpha \log \left(\frac{\rho_\infty(z)}{\tilde{\rho}(z)} \right) + W * \rho_\infty(z) \right) = 0 \quad \forall z \in \text{supp}(\rho_\infty), \quad (12a)$$

$$\nabla_x \left(\int f_1(z, x) d\rho_\infty(z) + \int f_2(z, x) d\tilde{\rho}(z) + \frac{\beta}{2} \|x - x_0\|^2 \right) = 0 \quad \forall x \in \text{supp}(\mu_\infty) \quad (12b)$$

737 in the sense of distributions.

738 **Definition 9** (Steady states for (4)). Let $\rho_\infty \in L^1_+(\mathbb{R}^d) \cap L^\infty_{loc}(\mathbb{R}^d)$ with $\|\rho_\infty\|_1 = 1$. Then ρ_∞ is a steady
 739 state for the system (4) if $\rho_\infty \in W^{1,2}_{loc}(\mathbb{R}^d)$, $\nabla W * \rho_\infty \in L^1_{loc}(\mathbb{R}^d)$, ρ_∞ is absolutely continuous with respect
 740 to $\tilde{\rho}$, and ρ_∞ satisfies

$$\nabla_z \left(f_1(z, b(\rho_\infty)) - \alpha \log \left(\frac{\rho_\infty(z)}{\tilde{\rho}(z)} \right) - W * \rho_\infty(z) \right) = 0 \quad \forall z \in \mathbb{R}^d, \quad (13)$$

741 in the sense of distributions, where $b(\rho_\infty) := \text{argmin}_x G_c(\rho_\infty, x)$.

742 **Definition 10** (Steady states for (5)). *The vector $x_\infty \in \mathbb{R}^d$ is a steady state for the system (5) if it satisfies*

$$\nabla_x G_d(x_\infty) = 0.$$

743 In fact, with the above notions of steady state, we can obtain improved regularity for ρ_∞ .

744 **Lemma 8.** *Assume $\tilde{\rho} \in C^1(\mathbb{R}^d)$. Then the steady states ρ_∞ for (3) and (4) are continuous.*

745 *Proof.* We present here the argument for equation (4) only. The result for (3) follows in exactly the same way
746 by replacing $f_1(z, b(\rho_\infty))$ with $-\int f_1(z, x) d\mu_\infty(x)$.

747 Thanks to our assumptions, we have $f_1(\cdot, b(\rho_\infty)) + \alpha \log \tilde{\rho}(\cdot) \in C^1$, which implies that $\nabla(f_1(\cdot, b(\rho_\infty)) +$
748 $\alpha \log \tilde{\rho}(\cdot)) \in L_{loc}^\infty$. By the definition of a steady state, $\rho_\infty \in L^1 \cap L_{loc}^\infty$ and thanks to Assumption 3 we have
749 $W \in C^2$, which implies that $\nabla W * \rho_\infty \in L_{loc}^\infty$. Let

$$h(z) := \rho_\infty(z) \nabla [f_1(z, b(\rho_\infty)) + \alpha \log \tilde{\rho}(z) - (W * \rho_\infty)(z)].$$

750 Then by the aforementioned regularity, we obtain $h \in L_{loc}^1 \cap L_{loc}^\infty$. By interpolation, it follows that $h \in L_{loc}^p$ for
751 all $1 < p < \infty$. This implies that $\operatorname{div}(\rho_\infty h) \in W_{loc}^{-1,p}$. Since ρ_∞ is a weak $W_{loc}^{1,2}$ -solution of (13), we have

$$\Delta \rho_\infty = \operatorname{div}(\rho_\infty h),$$

752 and so by classic elliptic regularity theory we conclude $\rho_\infty \in W_{loc}^{1,p}$. Finally, applying Morrey's inequality, we
753 have $\rho_\infty \in C^{0,k}$ where $k = \frac{p-d}{p}$ for any $d < p < \infty$. Therefore $\rho_\infty \in C(\mathbb{R}^d)$ (after possibly being redefined
754 on a set of measure zero). \square

755 B Proof of Theorem 1

756 For ease of notation, we write $G_a : \mathcal{P}(\mathbb{R}^d) \times \mathcal{P}(\mathbb{R}^d) \mapsto [0, \infty]$ as

$$G_a((\rho, \mu)) = \alpha KL(\rho|\tilde{\rho}) + \mathcal{V}(\rho, \mu) + \mathcal{W}(\rho),$$

757 where we define

$$\begin{aligned} \mathcal{V}(\rho, \mu) &= \iint f_1(z, x) d\rho(z) d\mu(x) + \int V(x) d\mu(x), \\ \mathcal{W}(\rho) &= \frac{1}{2} \iint W(z_1 - z_2) d\rho(z_1) d\rho(z_2), \end{aligned}$$

758 with potential given by $V(x) := \int f_2(z, x) d\tilde{\rho}(z) + \frac{\beta}{2} \|x - x_0\|^2$.

759 In order to prove the existence of a unique ground state for G_a , a natural approach is to consider the corresponding
760 Euler-Lagrange equations

$$\alpha \log \frac{\rho(z)}{\tilde{\rho}(z)} + \int f_1(z, x) d\mu(x) + (W * \rho)(z) = c_1[\rho, \mu] \quad \text{for all } z \in \operatorname{supp}(\rho), \quad (14a)$$

$$\int f_1(z, x) d\rho(z) + V(x) = c_2[\rho, \mu] \quad \text{for all } x \in \operatorname{supp}(\mu), \quad (14b)$$

761 where c_1, c_2 are constants that may differ on different connected components of $\operatorname{supp}(\rho)$ and $\operatorname{supp}(\mu)$. These
762 equations are not easy to solve explicitly, and we are therefore using general non-constructive techniques from
763 calculus of variations. We first show continuity and convexity properties for the functional G_a (Lemma 9 and
764 Proposition 10), essential properties that will allow us to deduce existence and uniqueness of ground states
765 using the direct method in the calculus of variations (Proposition 11). Using the Euler-Lagrange equation 14,
766 we then prove properties on the support of the ground state (Corollary 12). To obtain convergence results,
767 we apply the HWI method: we first show a general 'interpolation' inequality between the energy, the energy
768 dissipation and the metric (Proposition 13); this fundamental inequality will then imply a generalized logarithmic
769 Sobolev inequality (Corollary 14) relating the energy to the energy dissipation, and a generalized Talagrand
770 inequality (Corollary 15 that allows to translate convergence in energy into convergence in metric. Putting all
771 these ingrediends together will then allow us to conclude for the statements in Theorem 1.

772 **Lemma 9.** *The functional $G_a : \mathcal{P} \times \mathcal{P} \rightarrow \mathbb{R}$ is lower semi-continuous with respect to the weak-* topology.*

773 *Proof.* We split the energy G_a into three parts: (i) $KL(\rho|\tilde{\rho})$, (ii) the interaction energy \mathcal{W} , and (iii) the potential
774 energy \mathcal{V} . For (i), lower semi-continuity has been shown in [Pos75]. For (ii), we can directly apply [San15b,
775 Proposition 7.2] using Assumption 3. For (iii), note that V and f_1 are lower semi-continuous and bounded below
776 thanks to Assumption 1, and so the result follows from [San15b, Proposition 7.1]. \square

777 **Proposition 10** (Uniform displacement convexity). *Let $\alpha > 0$ and $\beta > 0$. Fix $\gamma_0, \gamma_1 \in \mathcal{P}_2 \times \mathcal{P}_2$ and let*
778 *Assumptions 1,2 and 3 hold. Along any geodesic $(\gamma_s)_{s \in [0,1]} \in \mathcal{P}_2 \times \mathcal{P}_2$ connecting γ_0 to γ_1 , we have for all*
779 *$s \in [0, 1]$*

$$\frac{d^2}{ds^2} G_a(\gamma_s) \geq \eta \bar{W}(\gamma_0, \gamma_1)^2, \quad \eta := \lambda_1 + \min(\lambda_2 + \beta, \alpha \tilde{\lambda}). \quad (15)$$

780 *As a result, the functional $G_a : \mathcal{P} \times \mathcal{P} \rightarrow \mathbb{R}$ is uniformly displacement convex with constant $\eta > 0$.*

781 *Proof.* Let γ_0 and γ_1 be two probability measures with bounded second moments. Denote by $\phi, \psi : \mathbb{R}^d \rightarrow \mathbb{R}$
782 the optimal Kantorovich potentials pushing ρ_0 onto ρ_1 , and μ_0 onto μ_1 , respectively:

$$\begin{aligned} \rho_1 = \nabla \phi_{\#} \rho_0 \quad \text{such that} \quad W_2(\rho_0, \rho_1)^2 &= \int_{\mathbb{R}^d} \|z - \nabla \phi(z)\|^2 d\rho_0(z), \\ \mu_1 = \nabla \psi_{\#} \mu_0 \quad \text{such that} \quad W_2(\mu_0, \mu_1)^2 &= \int_{\mathbb{R}^d} \|x - \nabla \psi(x)\|^2 d\mu_0(x). \end{aligned}$$

783 The now classical results in [BB00] guarantee that there always exists convex functions ϕ, ψ that satisfy the
784 conditions above. Then the path $(\gamma_s)_{s \in [0,1]} = (\rho_s, \mu_s)_{s \in [0,1]}$ defined by

$$\begin{aligned} \rho_s &= [(1-s) \text{id} + s \nabla_z \phi]_{\#} \rho_0, \\ \mu_s &= [(1-s) \text{id} + s \nabla_x \psi]_{\#} \mu_0 \end{aligned}$$

785 is a \bar{W} -geodesic from γ_0 to γ_1 .

786 The first derivative of \mathcal{V} along geodesics in the Wasserstein metric is given by

$$\begin{aligned} \frac{d}{ds} \mathcal{V}(\gamma_s) &= \frac{d}{ds} \left[\iint f_1((1-s)z + s \nabla \phi(z), (1-s)x + s \nabla \psi(x)) d\rho_0(z) d\mu_0(x) \right. \\ &\quad \left. + \int V((1-s)x + s \nabla \psi(x)) d\mu_0(x) \right] \\ &= \iint \nabla_x f_1((1-s)z + s \nabla \phi(z), (1-s)x + s \nabla \psi(x)) \cdot (\nabla \psi(x) - x) d\rho_0(z) d\mu_0(x) \\ &\quad + \iint \nabla_z f_1((1-s)z + s \nabla \phi(z), (1-s)x + s \nabla \psi(x)) \cdot (\nabla \phi(z) - z) d\rho_0(z) d\mu_0(x) \\ &\quad + \int \nabla_x V((1-s)x + s \nabla \psi(x)) \cdot (\nabla \psi(x) - x) d\mu_0(x), \end{aligned}$$

787 and taking another derivative we have

$$\begin{aligned} \frac{d^2}{ds^2} \mathcal{V}(\gamma_s) &= - \iint \left[\begin{array}{c} (\nabla \psi(x) - x) \\ (\nabla \phi(z) - z) \end{array} \right]^T \cdot D_s(z, x) \cdot \left[\begin{array}{c} (\nabla \psi(x) - x) \\ (\nabla \phi(z) - z) \end{array} \right] d\rho_0(z) d\mu_0(x) \\ &\quad + \iint (\nabla \psi(x) - x)^T \cdot \nabla_x^2 V((1-s)x + s \nabla \psi(x)) \cdot (\nabla \psi(x) - x) d\rho_0(z) d\mu_0(x) \\ &\geq \lambda_1 \bar{W}(\gamma_0, \gamma_1)^2 + (\lambda_2 + \beta) W_2(\mu_0, \mu_1)^2, \end{aligned}$$

788 where we denoted $D_s(z, x) := \text{Hess}(f_1)((1-s)z + s \nabla \phi(z), (1-s)x + s \nabla \psi(x))$, and the last inequality
789 follows from Assumption 1 and the optimality of the potentials ϕ and ψ .

790 Following [CMV03; Vil03b] and using Assumption 2, the second derivatives of the diffusion term and the
791 interaction term along geodesics are given by

$$\frac{d^2}{ds^2} KL(\rho_s | \tilde{\rho}) \geq \alpha \tilde{\lambda} W_2(\rho_0, \rho_1)^2, \quad \frac{d^2}{ds^2} \mathcal{W}(\rho_s) \geq 0. \quad (16)$$

792 Putting the above estimates together, we obtain (15).

793 □

794 **Remark 5.** *Alternatively, one could assume strong convexity of W , which would improve the lower-bound on*
795 *the second derivative along geodesics.*

796 **Proposition 11.** (Ground state) *Let Assumptions 1-3 hold for $\alpha, \beta > 0$. Then the functional $G_a : \mathcal{P}(\mathbb{R}^d) \times$
797 $\mathcal{P}(\mathbb{R}^d) \rightarrow [0, \infty]$ admits a unique minimizer $\gamma_* = (\rho_*, \mu_*)$, and it satisfies $\rho_* \in \mathcal{P}_2(\mathbb{R}^d) \cap L^1(\mathbb{R}^d)$, $\mu_* \in$
798 $\mathcal{P}_2(\mathbb{R}^d)$, and ρ_* is absolutely continuous with respect to $\tilde{\rho}$.*

799 *Proof.* We show existence of a minimizer of G_a using the direct method in the calculus of variations. Denote by
800 $\gamma = (\rho, \mu) \in \mathcal{P} \times \mathcal{P} \subset \mathcal{M} \times \mathcal{M}$ a pair of probability measures as a point in the product space of Radon measures.
801 Since $G_a \geq 0$ on $\mathcal{P} \times \mathcal{P}$ (see Assumption 1) and not identically $+\infty$ everywhere, there exists a minimizing
802 sequence $(\gamma_n) \in \mathcal{P} \times \mathcal{P}$. Note that (γ_n) is in the closed unit ball of the dual space of continuous functions
803 vanishing at infinity $(C_0(\mathbb{R}^d) \times C_0(\mathbb{R}^d))^*$ endowed with the dual norm $\|\gamma_n\|_* = \sup \frac{|\int f d\rho_n + \int g d\mu_n|}{\|(f, g)\|_\infty}$ over
804 $f, g \in C_0(\mathbb{R}^d)$ with $\|(f, g)\|_\infty := \|f\|_\infty + \|g\|_\infty \neq 0$. By the Banach-Alaoglu theorem [Rud91, Thm 3.15]
805 there exists a limit $\gamma_* = (\rho_*, \mu_*) \in \mathcal{M} \times \mathcal{M} = (C_0 \times C_0)^*$ and a convergent subsequence (not relabelled)
806 such that $\gamma_n \xrightarrow{*} \gamma_*$. In fact, ρ_* is absolutely continuous with respect to $\tilde{\rho}$ implying $\rho_* \in L^1(\mathbb{R}^d)$ thanks to
807 Assumption 2. Further, μ_* has bounded second moment, else we would have $\inf_{\gamma \in \mathcal{P} \times \mathcal{P}} G_a(\gamma) = \infty$ which
808 yields a contradiction. It remains to show that $\int d\rho_* = \int d\mu_* = 1$ to conclude that $\gamma_* \in \mathcal{P} \times \mathcal{P}$. To this
809 aim, it is sufficient to show tightness of (ρ_n) and (μ_n) , preventing the escape of mass to infinity as we have
810 $\int d\rho_n = \int d\mu_n = 1$ for all $n \geq 1$. Tightness follows from Markov's inequality [Gho02] if we can establish
811 uniform bounds on the second moments, i.e. we want to show that there exists a constant $C > 0$ independent of
812 n such that

$$\int \|z\|^2 d\rho_n(z) + \int \|x\|^2 d\mu_n(x) < C \quad \forall n \in \mathbb{N}. \quad (17)$$

813 To establish (17), observe that thanks to Assumption 2, there exists a constant $c_0 \in \mathbb{R}$ (possibly negative) such
814 that $-\log \tilde{\rho}(z) \geq c_0 + \frac{\tilde{\lambda}}{4} \|z\|^2$ for all $z \in \mathbb{R}^d$. Then

$$\frac{\alpha \tilde{\lambda}}{4} \int \|z\|^2 d\rho_n \leq -\alpha c_0 - \alpha \int \log \tilde{\rho}(z) d\rho_n$$

815 Therefore, using $\int d\rho_n = \int d\mu_n = 1$ and writing $\zeta := \min\{\frac{\alpha \tilde{\lambda}}{4}, \frac{\beta}{2}\} > 0$, we obtain the desired uniform upper
816 bound on the second moments of the minimizing sequence,

$$\begin{aligned} \zeta \iint (\|z\|^2 + \|x\|^2) d\rho_n d\mu_n &\leq -\alpha c_0 - \alpha \int \log \tilde{\rho}(z) d\rho_n + \beta \int \|x - x_0\|^2 d\mu_n + \beta \|x_0\|^2 \\ &\leq -\alpha c_0 + \beta \|x_0\|^2 + G_a(\gamma_n) \\ &\leq -\alpha c_0 + \beta \|x_0\|^2 + G_a(\gamma_1) < \infty. \end{aligned}$$

817 This concludes the proof that the limit γ_* satisfies indeed $\gamma_* \in \mathcal{P} \times \mathcal{P}$, and indeed $\rho_* \in \mathcal{P}_2(\mathbb{R}^d)$ as well. Finally,
818 γ_* is indeed a minimizer of G_a thanks to weak-* lower-semicontinuity of G_a following Lemma 9.

819 Next we show uniqueness using a contradiction argument. Suppose $\gamma_* = (\rho_*, \mu_*)$ and $\gamma'_* = (\rho'_*, \mu'_*)$ are
820 minimizers of G_a . For $t \in [0, 1]$, define $\gamma_t := ((1-t)\text{id} + tT, (1-t)\text{id} + tS)_{\#} \gamma_*$, where $T, S : \mathbb{R}^d \mapsto \mathbb{R}^d$
821 are the optimal transport maps such that $\rho'_* = T_{\#} \rho_*$ and $\mu'_* = S_{\#} \mu_*$. By Proposition 10 the energy G_a is
822 uniformly displacement convex, and so we have

$$G_a(\gamma_t) \leq (1-t)G_a(\gamma_*) + tG_a(\gamma'_*) = G_a(\gamma_*).$$

823 If $\gamma_* \neq \gamma'_*$ and $t \in (0, 1)$, then strict inequality holds by applying similar arguments as in [McC97, Proposition
824 1.2]. However, if $\gamma_* \neq \gamma'_*$, the strict inequality $G_a(\gamma_t) < G_a(\gamma_*)$ is a contradiction to the minimality of γ_* .
825 Hence, the minimizer is unique. \square

826 **Remark 6.** If $\lambda_1 > 0$, then the strict convexity of f_1 can be used to deduce uniqueness, and the assumptions on
827 $-\log \tilde{\rho}$ can be weakened from strict convexity to convexity.

828 **Corollary 12.** Any minimizer $\gamma_* = (\rho_*, \mu_*)$ of G_a is a steady state for equation (3) according to Definition 8
829 and satisfies $\text{supp}(\rho_*) = \text{supp}(\tilde{\rho})$.

830 *Proof.* By Proposition 11, we have $\rho_* \in L^1_+$, $\|\rho_*\|_1 = 1$, $\mu_* \in \mathcal{P}_2$ and that ρ_* is absolutely continuous with
831 respect to $\tilde{\rho}$. Since $W \in C^2(\mathbb{R}^d)$, it follows that $\nabla W * \rho_* \in L^1_{loc}$. In order to show that γ_* is a steady state for
832 equation (3), it remains to prove that $\rho_* \in W^{1,2}_{loc} \cap L^\infty_{loc}$. As γ_* is a minimizer, it is in particular a critical point,
833 and therefore satisfies equations (14). Rearranging, we obtain (for a possible different constant $c_1[\rho_*, \mu_*] \neq 0$)
834 from (14a) that

$$\rho_*(z) = c_1[\rho_*, \mu_*] \tilde{\rho}(z) \exp \left[-\frac{1}{\alpha} \left(\int f_1(z, x) \mu_*(x) + W * \rho_*(z) \right) \right] \quad \text{on } \text{supp}(\rho_*). \quad (18)$$

835 Then for any compact set $K \subset \mathbb{R}^d$,

$$\sup_{z \in K} \rho_*(z) \leq c_1[\rho_*, \mu_*] \sup_{z \in K} \tilde{\rho}(z) \sup_{z \in K} \exp \left(-\frac{1}{\alpha} \left(\int f_1(z, x) \mu_*(x) \right) \right) \sup_{z \in K} \exp \left(-\frac{1}{\alpha} W * \rho_* \right).$$

836 As $f_1 \geq 0$ by Assumption 1 and $W \geq 0$ by Assumption 3, the last two terms are finite. The first supremum
837 is finite thanks to continuity of $\tilde{\rho}$. Therefore $\rho_* \in L^\infty_{loc}$. To show that $\rho_* \in W^{1,2}_{loc}$, note that for any compact

838 set $K \subset \mathbb{R}^d$, we have $\int_K |\rho_*(z)|^2 dz < \infty$ as a consequence of $\rho_* \in L_{loc}^\infty$. Moreover, defining $T[\gamma](z) :=$
839 $-\frac{1}{\alpha} (\int f_1(z, x) \mu(x) + W * \rho(z)) \leq 0$, we have

$$\begin{aligned} \int_K |\nabla \rho_*|^2 dz &= c_1 [\rho_*, \mu_*]^2 \int_K |\nabla \tilde{\rho} + \tilde{\rho} \nabla T[\gamma_*]|^2 \exp(2T[\gamma_*]) dz \\ &\leq 2c_1 [\rho_*, \mu_*]^2 \int_K |\nabla \tilde{\rho}|^2 \exp(2T[\gamma_*]) dz + 2c_1 [\rho_*, \mu_*]^2 \int_K |\nabla T[\gamma_*]|^2 \tilde{\rho}^2 \exp(2T[\gamma_*]) dz, \end{aligned}$$

840 which is bounded noting that $\exp(2T[\gamma_*]) \leq 1$ and that $T[\gamma_*](\cdot)$, $\nabla T[\gamma_*](\cdot)$ and $\nabla \tilde{\rho}$ are in L_{loc}^∞ , where we used
841 that $f_1, (\cdot, x), W(\cdot), \tilde{\rho}(\cdot) \in C^1(\mathbb{R}^d)$ by Assumptions 1-3. We conclude that $\rho_* \in W_{loc}^{1,2}$, and indeed (ρ_*, μ_*)
842 solves (12) in the sense of distributions as a consequence of (14).

Next, we show that $\text{supp}(\rho_*) = \text{supp}(\tilde{\rho})$ using again the relation (18). Firstly, note that $\text{supp}(\rho_*) \subset \text{supp}(\tilde{\rho})$ since ρ_* is absolutely continuous with respect to $\tilde{\rho}$. Secondly, we claim that $\exp[-\frac{1}{\alpha} (\int f_1(z, x) \mu_*(x) + W * \rho_*(z))] > 0$ for all $z \in \mathbb{R}^d$. In other words, we claim that $\int f_1(z, x) \mu_*(x) < \infty$ and $W * \rho_*(z) < \infty$ for all $z \in \mathbb{R}^d$. Indeed, for the first term, fix any $z \in \mathbb{R}^d$ and choose $R > 0$ large enough such that $z \in B_R(0)$. Then, thanks to continuity of f_1 according to Assumption 1, we have

$$\int f_1(z, x) \mu_*(x) \leq \sup_{z \in B_R(0)} \int f_1(z, x) \mu_*(x) < \infty.$$

843 For the second term, note that by Assumption 3, we have for any $z \in \mathbb{R}^d$ and $\epsilon > 0$,

$$\begin{aligned} W(z) &\leq W(0) + \nabla W(z) \cdot z \leq W(0) + \frac{1}{2\epsilon} \|\nabla W(z)\|^2 + \frac{\epsilon}{2} \|z\|^2 \\ &\leq W(0) + \frac{D^2}{2\epsilon} (1 + \|z\|)^2 + \frac{\epsilon}{2} \|z\|^2 \leq W(0) + \frac{D^2}{\epsilon} + \left(\frac{D^2}{\epsilon} + \frac{\epsilon}{2}\right) \|z\|^2 \\ &= W(0) + \frac{D}{\sqrt{2}} + \sqrt{2}D \|z\|^2, \end{aligned}$$

844 where the last equality follows by choosing the optimal $\epsilon = \sqrt{2}D$. We conclude that

$$\begin{aligned} W * \rho_*(z) &\leq W(0) + \frac{D}{\sqrt{2}} + \sqrt{2}D \int \|z - \tilde{z}\|^2 \rho_*(\tilde{z}) \\ &\leq W(0) + \frac{D}{\sqrt{2}} + 2\sqrt{2}D \|z\|^2 + 2\sqrt{2}D \int \|\tilde{z}\|^2 \rho_*(\tilde{z}), \end{aligned} \quad (19)$$

845 which is finite for any fixed $z \in \mathbb{R}^d$ thanks to the fact that $\rho_* \in \mathcal{P}_2(\mathbb{R}^d)$. Hence, $\text{supp}(\rho_*) = \text{supp}(\tilde{\rho})$. \square

846 **Remark 7.** If we have in addition that $\tilde{\rho} \in L^\infty(\mathbb{R}^d)$, then the minimizer ρ_* of G_α is in $L^\infty(\mathbb{R}^d)$ as well. This
847 follows directly by bounding the right-hand side of (18).

848 The following inequality is referred to as HWI inequality and represents the key result to obtain convergence to
849 equilibrium.

850 **Proposition 13** (HWI inequality). *Define the dissipation functional*

$$D_\alpha(\gamma) := \iint |\delta_\gamma G_\alpha(z, x)|^2 d\gamma(z, x).$$

851 Assume $\alpha, \beta > 0$ and let η as defined in (15). Let $\gamma_0, \gamma_1 \in \mathcal{P}_2$ such that $G_\alpha(\gamma_0), G_\alpha(\gamma_1), D_\alpha(\gamma_0) < \infty$.
852 Then

$$G_\alpha(\gamma_0) - G_\alpha(\gamma_1) \leq \overline{W}(\gamma_0, \gamma_1) \sqrt{D_\alpha(\gamma_0)} - \frac{\eta}{2} \overline{W}(\gamma_0, \gamma_1)^2 \quad (20)$$

853 *Proof.* For simplicity, consider γ_0, γ_1 that have smooth Lebesgue densities of compact support. The general
854 case can be recovered using approximation arguments. Let $(\gamma_s)_{s \in [0,1]}$ denote a \overline{W} -geodesic between γ_0, γ_1 .
855 Following similar arguments as in [CMV03] and [OV00, Section 5] and making use of the calculations in the
856 proof of Proposition 10, we have

$$\frac{d}{ds} G_\alpha(\gamma_s) \Big|_{s=0} \geq \iint \begin{bmatrix} \xi_1(z) \\ \xi_2(x) \end{bmatrix} \cdot \begin{bmatrix} (\nabla \phi(z) - z) \\ (\nabla \psi(x) - x) \end{bmatrix} d\gamma_0(z, x),$$

857 where

$$\begin{aligned} \xi_1[\gamma_0](z) &:= \alpha \nabla_z \log \left(\frac{\rho_0(z)}{\tilde{\rho}(z)} \right) + \int \nabla_z f_1(z, x) d\mu_0(x) + \int \nabla_z W(z - z') d\rho_0(z'), \\ \xi_2[\gamma_0](x) &:= \int \nabla_x f_1(z, x) d\rho_0(z) + \nabla_x V(x). \end{aligned}$$

Note that the dissipation functional can then be written as

$$D_a(\gamma_0) = \iint (|\xi_1(z)|^2 + |\xi_2(x)|^2) d\gamma_0(z, x).$$

858 Using the double integral Cauchy-Schwarz inequality [Ste04], we obtain

$$\begin{aligned} \left. \frac{d}{ds} G_a(\gamma_s) \right|_{s=0} &\geq - \left(\sqrt{\iint \left\| \begin{bmatrix} \xi_1 \\ \xi_2 \end{bmatrix} \right\|_2^2 d\gamma_0} \right) \left(\sqrt{\iint \left\| \begin{bmatrix} \nabla\phi(z) - z \\ \nabla\psi(x) - x \end{bmatrix} \right\|_2^2 d\gamma_0} \right) \\ &= -\sqrt{D_a(\gamma_0)} \sqrt{\int \|\nabla\phi(z) - z\|^2 d\rho_0 + \int \|\nabla\psi(x) - x\|^2 d\mu_0} \\ &= -\sqrt{D_a(\gamma_0)} \overline{W}(\gamma_0, \gamma_1). \end{aligned}$$

859 Next, we compute a Taylor expansion of $G_a(\gamma_s)$ when considered as a function in s and use the bound on

860 $\frac{d^2}{ds^2} G_a$ from (15):

$$\begin{aligned} G_a(\gamma_1) &= G_a(\gamma_0) + \left. \frac{d}{ds} G_a(\gamma_s) \right|_{s=0} + \int_0^1 (1-t) \left(\left. \frac{d^2}{ds^2} G_a(\gamma_s) \right) \right|_{s=t} dt \\ &\geq G_a(\gamma_0) - \sqrt{D_a(\gamma_0)} \overline{W}(\gamma_0, \gamma_1) + \frac{\eta}{2} \overline{W}(\gamma_0, \gamma_1)^2. \end{aligned}$$

861

□

862 **Remark 8.** The HWI inequality in Proposition 13 immediately implies uniqueness of minimizers for G_a in the
863 set $\{\gamma \in \mathcal{P} \times \mathcal{P} : D_a(\gamma) < +\infty\}$. Indeed, if γ_0 is such that $D_a(\gamma_0) = 0$, then for any other γ_1 in the above
864 set we have $G_a(\gamma_0) \leq G_a(\gamma_1)$ with equality if and only if $\overline{W}(\gamma_0, \gamma_1) = 0$.

865 **Corollary 14** (Generalized Log-Sobolev inequality). Denote by γ_* the unique minimizer of G_a . With η as
866 defined in (15), any product measure $\gamma \in \mathcal{P}_2 \times \mathcal{P}_2$ such that $G(\gamma), D_a(\gamma) < \infty$ satisfies

$$D_a(\gamma) \geq 2\eta G_a(\gamma | \gamma_*). \quad (21)$$

867 *Proof.* This statement follows immediately from Proposition 13. Indeed, let $\gamma_1 = \gamma_*$ and $\gamma_0 = \gamma$ in (20). Then

$$\begin{aligned} G_a(\gamma | \gamma_*) &\leq \overline{W}(\gamma, \gamma_*) \sqrt{D_a(\gamma)} - \frac{\eta}{2} \overline{W}(\gamma, \gamma_*)^2 \\ &\leq \max_{t \geq 0} \left(\sqrt{D_a(\gamma)} t - \frac{\eta}{2} t^2 \right) = \frac{D_a(\gamma)}{2\eta}. \end{aligned}$$

868

□

Corollary 15 (Talagrand inequality). Denote by γ_* the unique minimizer of G_a . With η as defined in (15), it holds

$$\overline{W}(\gamma, \gamma_*)^2 \leq \frac{2}{\eta} G_a(\gamma | \gamma_*)$$

869 for any $\gamma \in \mathcal{P}_2 \times \mathcal{P}_2$ such that $G_a(\gamma) < \infty$.

870 *Proof.* This is also a direct consequence of Proposition 13 by setting $\gamma_0 = \gamma_*$ and $\gamma_1 = \gamma$. Then $G_a(\gamma_*) < \infty$
871 and $D_a(\gamma_*) = 0$, and the result follows. □

872 *Proof of Theorem 1.* The entropy term $\int \rho \log \rho$ produces diffusion in ρ for the corresponding PDE in (3). As a
873 consequence, solutions ρ_t to (3) and minimizers ρ^* for G_a have to be L^1 functions. As there is no diffusion for
874 the evolution of μ_t , solutions may have a singular part. In fact, for initial condition $\mu_0 = \delta_{x_0}$, the corresponding
875 solution will be of the form $\mu_t = \delta_{x(t)}$, where $x(t)$ solves the ODE (2) with initial condition x_0 . This follows
876 from the fact that the evolution for μ_t is a transport equation (also see Section A.1 for more details). Results (a)
877 and (b) are the statements in Proposition 11, Corollary 12 and Corollary 15. To obtain (c), we differentiate the
878 energy G_a along solutions γ_t to the equation (3):

$$\begin{aligned} \frac{d}{dt} G_a(\gamma_t) &= \int \delta_\rho G_a[\gamma_t](z) \partial_t \rho_t dz + \int \delta_\mu G_a[\gamma_t](x) \partial_t \mu_t dx \\ &= - \int \|\nabla_z \delta_\rho G_a[\gamma_t](z)\|^2 d\rho_t(z) - \int \|\nabla_x \delta_\mu G_a[\gamma_t](x)\|^2 d\mu_t(x) \\ &= -D_a(\gamma_t) \leq -2\eta G_a(\gamma_t | \gamma_*), \end{aligned}$$

879 where the last bound follows from Corollary 14. Applying Gronwall's inequality, we immediately obtain decay
880 in energy,

$$G_a(\gamma_t | \gamma_*) \leq e^{-2\eta t} G_a(\gamma_0 | \gamma_*).$$

881 Finally, applying Talagrand's inequality (Corollary 15), the decay in energy implies decay in the product
882 Wasserstein metric,

$$\overline{W}(\gamma_t, \gamma_*) \leq ce^{-\eta t}$$

883 where $c > 0$ is a constant only depending on γ_0, γ_* and the parameter η . □

884 C Proof of Theorem 2

885 In the case of competing objectives, we rewrite the energy $G_c(\rho, x) : \mathcal{P}(\mathbb{R}^d) \times \mathbb{R}^d \mapsto [-\infty, \infty]$ as follows:

$$G_c(\rho, x) = \int f_1(z, x) d\rho(z) + \int f_2(z, x) d\bar{\rho}(z) + \frac{\beta}{2} \|x - x_0\|^2 - P(\rho),$$

886 where

$$P(\rho) := \alpha KL(\rho | \bar{\rho}) + \frac{1}{2} \int \rho W * \rho.$$

Note that for any fixed $\rho \in \mathcal{P}$, the energy $G_c(\rho, \cdot)$ is strictly convex in x , and therefore has a unique minimizer. Define the best response by

$$b(\rho) := \operatorname{argmin}_{\bar{x}} G_c(\rho, \bar{x})$$

887 and denote $G_b(\rho) := G_c(\rho, b(\rho))$. We begin with an auxiliary result computing the first variations of the
888 different terms in $G_b(\rho)$ using Definition A.2.

889 **Lemma 16** (First variation of G_b). *The first variation of G_b is given by*

$$\delta_\rho G_b[\rho](z) = h_1(z) + h_2(z) + \beta h_3(z) - \delta_\rho P[\rho](z),$$

890 where

$$\begin{aligned} h_1(z) &:= \frac{\delta}{\delta \rho} \left(\int f_1(\bar{z}, b(\rho)) d\rho(\bar{z}) \right) (z) = \left\langle \int \nabla_x f_1(\bar{z}, b(\rho)) d\rho(\bar{z}), \frac{\delta b}{\delta \rho}[\rho](z) \right\rangle + f_1(z, b(\rho)), \\ h_2(z) &:= \frac{\delta}{\delta \rho} \left(\int f_2(\bar{z}, b(\rho)) d\bar{\rho}(\bar{z}) \right) (z) = \left\langle \int \nabla_x f_2(\bar{z}, b(\rho)) d\bar{\rho}(\bar{z}), \frac{\delta b}{\delta \rho}[\rho](z) \right\rangle, \\ h_3(z) &:= \frac{1}{2} \frac{\delta}{\delta \rho} \|b(\rho) - x_0\|^2 = \left\langle b(\rho) - x_0, \frac{\delta b}{\delta \rho}[\rho](z) \right\rangle, \end{aligned}$$

891 and

$$\delta_\rho P[\rho](z) = \alpha \log(\rho(z)/\bar{\rho}(z)) + (W * \rho)(z).$$

892 *Proof.* We begin with general expressions for Taylor expansions of $b : \mathcal{P}(\mathbb{R}^d) \rightarrow \mathbb{R}^d$ and $f_i(z, b(\cdot)) : \mathcal{P}(\mathbb{R}^d) \rightarrow$
893 \mathbb{R} for $i = 1, 2$ around ρ . Let $\psi \in \mathcal{T}$ with $\mathcal{T} = \{\psi : \int \psi(z) dz = 0\}$. Then

$$b(\rho + \epsilon \psi) = b(\rho) + \epsilon \int \frac{\delta b}{\delta \rho}[\rho](z') \psi(z') dz' + O(\epsilon^2) \quad (22)$$

894 and

$$f_i(z, b(\rho + \epsilon \psi)) = f_i(z, b(\rho)) + \epsilon \left\langle \nabla_x f_i(z, b(\rho)), \int \frac{\delta b}{\delta \rho}[\rho](z') \psi(z') dz' \right\rangle + O(\epsilon^2). \quad (23)$$

895 We compute explicitly each of the first variations:

896 (i) Using (23), we have

$$\begin{aligned} \int \psi(z) h_1(z) dz &= \lim_{\epsilon \rightarrow 0} \frac{1}{\epsilon} \left[\int f_1(z, b(\rho + \epsilon \psi))(\rho(z) + \epsilon \psi(z)) dz - \int f_1(z, b(\rho)) \rho(z) dz \right] \\ &= \left\langle \int \nabla_x f_1(z, b(\rho)) d\rho(z), \int \frac{\delta b(\rho)}{\delta \rho}[\rho](z') \psi(z') dz' \right\rangle + \int f_1(z, b(\rho)) \psi(z) dz \\ &= \int \left\langle \int \nabla_x f_1(z, b(\rho)) d\rho(z), \frac{\delta b(\rho)}{\delta \rho}[\rho](z') \right\rangle \psi(z') dz' + \int f_1(z, b(\rho)) \psi(z) dz \\ &\Rightarrow h_1(z) = \left\langle \int \nabla_x f_1(\bar{z}, b(\rho)) d\rho(\bar{z}), \frac{\delta b}{\delta \rho}[\rho](z) \right\rangle + f_1(z, b(\rho)). \end{aligned}$$

897 (ii) Similarly, using again (23),

$$\begin{aligned} \int \psi(z) h_2(z) dz &= \lim_{\epsilon \rightarrow 0} \frac{1}{\epsilon} \left[\int f_2(z, b(\rho + \epsilon\psi)) d\bar{\rho}(z) - \int f_2(z, b(\rho)) \bar{\rho}(z) dz \right] \\ &= \int \left\langle \int \nabla_x f_2(\tilde{z}, b(\rho)) d\bar{\rho}(\tilde{z}), \frac{\delta b}{\delta \rho}[\rho](z) \right\rangle \psi(z) dz \\ \Rightarrow h_2(z) &= \left\langle \int \nabla_x f_2(\tilde{z}, b(\rho)) d\bar{\rho}(\tilde{z}), \frac{\delta b}{\delta \rho}[\rho](z) \right\rangle. \end{aligned}$$

898 (iii) Finally, from (22) it follows that

$$\begin{aligned} \int \psi(z) h_3(z) dz &= \lim_{\epsilon \rightarrow 0} \frac{1}{2\epsilon} \left[\langle b(\rho + \epsilon\psi) - x_0, b(\rho + \epsilon\psi) - x_0 \rangle - \langle b(\rho) - x_0, b(\rho) - x_0 \rangle \right] \\ &= \int \left\langle b(\rho) - x_0, \frac{\delta b}{\delta \rho}[\rho](z) \right\rangle \psi(z) dz \\ \Rightarrow h_3(z) &= \left\langle b(\rho) - x_0, \frac{\delta b}{\delta \rho}[\rho](z) \right\rangle. \end{aligned}$$

899 Finally, the expression for $\delta_\rho P[\rho]$ follows by direct computation □

900 **Lemma 17.** Denote $G_b(\rho) := G_c(\rho, b(\rho))$ with $b(\rho)$ given by (4). Then $\delta_\rho G_b[\rho] = \delta_\rho G_c[\rho]|_{x=b(\rho)}$.

901 *Proof.* We start by computing $\delta_\rho G_c(\cdot, x)[\rho](z)$ for any $z, x \in \mathbb{R}^d$:

$$\delta_\rho G_c(\cdot, x)[\rho](z) = f_1(z, x) - \delta_\rho P[\rho](z). \quad (24)$$

902 Next, we compute $\delta_\rho G_b$. Using Lemma 16, the first variation of G_b is given by

$$\begin{aligned} \delta_\rho G_b[\rho](z) &= h_1(z) + h_2(z) + \beta h_3(z) - \delta_\rho P[\rho](z) \\ &= - \left\langle \left[\int \nabla_x f_1(\tilde{z}, b(\rho)) d\rho(\tilde{z}) + \int \nabla_x f_2(\tilde{z}, b(\rho)) d\bar{\rho}(\tilde{z}) + \beta(b(\rho) - x_0) \right], \delta_\rho b[\rho](z) \right\rangle \\ &\quad + f_1(z, b(\rho)) - \delta_\rho P[\rho](z). \end{aligned}$$

903 Note that

$$\nabla_x G_c(\rho, x) = \int \nabla_x f_1(\tilde{z}, x) d\rho(\tilde{z}) + \int \nabla_x f_2(\tilde{z}, x) d\bar{\rho}(\tilde{z}) + \beta(x - x_0), \quad (25)$$

904 and by the definition of the best response $b(\rho)$, we have $\nabla_x G_x(\rho, x)|_{x=b(\rho)} = 0$. Substituting into the expression
905 for $\delta_\rho G_b$ and using (24), we obtain

$$\delta_\rho G_b[\rho](z) = f_1(z, b(\rho)) - \delta_\rho P[\rho](z) = \delta_\rho G_c(\cdot, x)[\rho](z) \Big|_{x=b(\rho)}.$$

906 This concludes the proof. □

907 **Lemma 18** (Uniform boundedness of the best response). *Let Assumption 1 hold. Then for any $\rho \in \mathcal{P}(\mathbb{R}^d)$, we*
908 *have*

$$\|b(\rho)\|^2 \leq \|x_0\|^2 + \frac{2(a_1 + a_2)}{\beta}.$$

Proof.

$$\int \nabla_x f_1(z, b(\rho)) d\rho_t + \int \nabla_x f_2(z, b(\rho)) d\bar{\rho}(z) + \beta(b(\rho) - x_0) = 0.$$

909 To show that that $b(\rho)$ is uniformly bounded, we take the inner product of the above expression with $b(\rho)$ itself

$$\beta \|b(\rho)\|^2 = \beta x_0 \cdot b(\rho) - \int \nabla_x f_1(z, b(\rho)) \cdot b(\rho) d\rho(z) - \int \nabla_x f_2(z, b(\rho)) \cdot b(\rho) d\bar{\rho}(z).$$

910 Using Assumption 1 to bound the two integrals, together with using Young's inequality to bound the first term
911 on the right-hand side, we obtain

$$\beta \|b(\rho)\|^2 \leq \frac{\beta}{2} \|x_0\|^2 + \frac{\beta}{2} \|b(\rho)\| + a_1 + a_2,$$

912 which concludes the proof after rearranging terms. □

913 **Lemma 19** (Upper semi-continuity). *The functionals $G_c : \mathcal{P}(\mathbb{R}^d) \times \mathbb{R}^d \rightarrow [-\infty, +\infty]$ is upper semi-continuous*
 914 *when $\mathcal{P}(\mathbb{R}^2) \times \mathbb{R}^d$ is endowed with the product topology of the weak-* topology and the Euclidean topology,*
 915 *and $G_b : \mathcal{P}(\mathbb{R}^d) \rightarrow [-\infty, +\infty]$ is upper semi-continuous with respect to the weak-* topology.*

916 *Proof.* The functional $G_c : \mathcal{P}(\mathbb{R}^d) \times \mathbb{R}^d \rightarrow [-\infty, +\infty]$ is continuous in the second variable thanks to
 917 Assumption 1. Similarly, $\int f_1(z, x) d\rho(z) + \int f_2(z, x) d\bar{\rho}(z)$ is continuous in ρ thanks to [San15b, Proposition
 918 7.1] using the continuity of f_1 and f_2 . Further, $-P$ is upper semi-continuous using [Pos75] and [San15b,
 919 Proposition 7.2] thanks to Assumptions 2 and 3. This concludes the continuity properties for G_c .

920 The upper semi-continuity of G_b then follows from a direct application of a version of Berge's maximum
 921 theorem [AB06, Lemma 16.30]. Let $R := \|x_0\|^2 + \frac{2(a_1+a_2)}{\beta} > 0$. We define $\varphi : (\mathcal{P}(\mathbb{R}^d), W_2) \rightarrow \mathbb{R}^d$
 922 as the correspondence that maps any $\rho \in \mathcal{P}(\mathbb{R}^d)$ to the closed ball $\overline{B_R(0)} \subset \mathbb{R}^d$. Then the graph of φ is
 923 $\text{Gr } \varphi = \mathcal{P}(\mathbb{R}^d) \times \{\overline{B_R(0)}\}$. With this definition of φ , the range of φ is compact and φ is continuous with respect
 924 to weak-* convergence, and so it is in particular upper hemicontinuous. Thanks to Lemma 18, the best response
 925 function $b(\rho)$ is always contained in $\overline{B_R(0)}$ for any choice of $\rho \in \mathcal{P}(\mathbb{R}^d)$. As a result, maximizing $-G_c(\rho, x)$
 926 in x over \mathbb{R}^d for a fixed $\rho \in \mathcal{P}(\mathbb{R}^d)$ reduces to maximizing it over $\overline{B_R(0)}$. Using the notation introduced above,
 927 we can restrict G_c to $G_c : \text{Gr } \varphi \rightarrow \mathbb{R}$ and write

$$G_b(\rho) := \max_{\hat{x} \in \varphi(\rho)} -G_c(\rho, \hat{x}).$$

928 Because $G_c(\rho, x)$ is upper semi-continuous when $\mathcal{P}(\mathbb{R}^2) \times \mathbb{R}^d$ is endowed with the product topology of the weak-
 929 * topology and the Euclidean topology, [AB06, Lemma 16.30] guarantees that $G_b(\cdot)$ is upper semi-continuous
 930 in the weak-* topology. \square

931 **Lemma 20** (First variation of the best response). *The first variation of the best response of the classifier at ρ is*

$$\delta_\rho b[\rho](z) = -Q(\rho)^{-1} \nabla_x f_1(z, b(\rho))$$

where $Q(\rho) \succeq (\beta + \lambda_1 + \lambda_2) \text{I}_d$ is a symmetric matrix, constant in z and x , defined as

$$Q(\rho) := \beta \text{I}_d + \int \nabla_x^2 f_1(z, b(\rho)) d\rho(z) + \int \nabla_x^2 f_2(z, b(\rho)) d\bar{\rho}(z).$$

932 *Proof.* We compute $\delta_\rho b[\rho](z)$ by using that any minimizer of $G_c(\rho, x)$ for fixed ρ must satisfy

$$\nabla_x G_c(\rho, b(\rho)) = 0.$$

933 Taking the first variation on the left-hand side (assuming it exists), we obtain

$$\delta_\rho \nabla_x G_c[\rho, b(\rho)] + \delta_\rho b[\rho](z) \nabla_x^2 G_c(\rho, b(\rho)) = 0.$$

934 Next, we explicitly compute all terms involved and show that $\nabla_x^2 G_c(\rho, b(\rho))$ is invertible. Computing the
 935 derivatives yields

$$\begin{aligned} \nabla_x G_c(\rho, x) &= \int \nabla_x f_1(z, x) d\rho(z) + \int \nabla_x f_2(z, x) d\bar{\rho}(z) + \beta(x - x_0) \\ \delta_\rho \nabla_x G_c[\rho, x](z) &= \nabla_x f_1(z, x) \\ \nabla_x^2 G_c(\rho, x) &= \int \nabla_x^2 f_1(z, x) d\rho(z) + \int \nabla_x^2 f_2(z, x) d\bar{\rho}(z) + \beta \text{I}_d. \end{aligned}$$

936 Note that $\nabla_x^2 G_c$ is invertible by Assumption 1, which states that f_1 and f_2 have positive-definite Hessians.
 937 Inverting this term and evaluating at $x = b(\rho)$ gives the first variation:

$$\delta_\rho b[\rho](z) = - \left[\beta \text{I}_d + \int \nabla_x^2 f_1(z, b(\rho)) d\rho(z) + \int \nabla_x^2 f_2(z, b(\rho)) d\bar{\rho}(z) \right]^{-1} \nabla_x f_1(z, b(\rho)).$$

938 The lower bound on $Q(\rho)$ also follows thanks to Assumption 1. \square

939 **Proposition 21.** *Let $\alpha, \beta > 0$ and assume Assumptions 1-4 hold with the parameters satisfying $\alpha\tilde{\lambda} > \Lambda_1$. Fix*
 940 *$\rho_0, \rho_1 \in \mathcal{P}(\mathbb{R}^d)$. Along any geodesic $(\rho_s)_{s \in [0,1]} \in \mathcal{P}_2(\mathbb{R}^d)$ connecting ρ_0 to ρ_1 , we have for all $s \in [0, 1]$*

$$\frac{d^2}{ds^2} G_b(\rho_s) \leq -\lambda_b W_1(\rho_0, \rho_1)^2, \quad \lambda_b := \alpha\tilde{\lambda} - \Lambda_1. \quad (26)$$

941 *As a result, the functional $G_b : \mathcal{P}_2(\mathbb{R}^d) \rightarrow [-\infty, +\infty]$ is uniformly displacement concave with constant $\lambda_b > 0$.*

942 *Proof.* Consider any $\rho_0, \rho_1 \in \mathcal{P}_2(\mathbb{R}^d)$. Then any W_2 -geodesic $(\rho_s)_{s \in [0,1]}$ connecting ρ_0 with ρ_1 solves the
 943 following system of geodesic equations:

$$\begin{cases} \partial_s \rho_s + \operatorname{div}(\rho_s v_s) = 0, \\ \partial_s(\rho_s v_s) + \operatorname{div}(\rho_s v_s \otimes v_s) = 0, \end{cases} \quad (27)$$

944 where $\rho_s : \mathbb{R}^d \rightarrow \mathbb{R}$ and $v_s : \mathbb{R}^d \mapsto \mathbb{R}^d$. The first derivative of G_b along geodesics can be computed explicitly
 945 as

$$\begin{aligned} \frac{d}{ds} G_b(\rho_s) &= \int \nabla_z f_1(z, b(\rho_s)) \cdot v_s(z) \rho_s(z) dz - \frac{d}{ds} P(\rho_s) \\ &+ \left\langle \left[\int \nabla_x f_1(z, x) d\rho_s(z) + \int \nabla_x f_2(z, x) d\bar{\rho}(z) + \beta(x - x_0) \right] \Big|_{x=b(\rho_s)}, \frac{d}{ds} b(\rho_s) \right\rangle. \end{aligned}$$

946 The left-hand side of the inner product is zero by definition of the best response $b(\rho_s)$ to ρ_s , see (25). Therefore

$$\frac{d}{ds} G_b(\rho_s) = \int \nabla_z f_1(z, b(\rho_s)) \cdot v_s(z) \rho_s(z) dz - \frac{d}{ds} P(\rho_s).$$

947 Differentiating a second time, using (27) and integration by parts, we obtain

$$\frac{d^2}{ds^2} G_b(\rho_s) = L_1(\rho_s) + L_2(\rho_s) - \frac{d^2}{ds^2} P(\rho_s),$$

948 where

$$\begin{aligned} L_1(\rho_s) &:= \int \nabla_z^2 f_1(z, b(\rho_s)) \cdot (v_s \otimes v_s) \rho_s dz = \int \langle v_s, \nabla_z^2 f_1(z, b(\rho_s)) \cdot v_s \rangle \rho_s dz, \\ L_2(\rho_s) &:= \int \frac{d}{ds} b(\rho_s) \cdot \nabla_x \nabla_z f_1(z, b(\rho_s)) \cdot v_s(z) \rho_s(z) dz. \end{aligned}$$

From (16), we have that

$$\frac{d^2}{ds^2} \tilde{P}(\rho_s) \geq \alpha \tilde{\lambda} W_2(\rho_0, \rho_1)^2,$$

949 and thanks to Assumption 4

950 we have

$$L_1(s) \leq \Lambda_1 W_2(\rho_0, \rho_1)^2.$$

951 This leaves L_2 to bound; we first consider the term $\frac{d}{ds} b(\rho_s)$:

$$\begin{aligned} \frac{d}{ds} b(\rho_s) &= \int \delta_\rho b[\rho_s](\tilde{z}) \partial_s \rho_s(d\tilde{z}) = - \int \delta_\rho b[\rho_s](\tilde{z}) \operatorname{div}(\rho_s v_s) d\tilde{z} \\ &= \int \nabla_z \delta_\rho b[\rho_s](\tilde{z}) \cdot v_s(\tilde{z}) d\rho_s(\tilde{z}). \end{aligned}$$

952 Defining $u(\rho_s) \in \mathbb{R}^d$ by

$$u(\rho_s) := \int \nabla_x \nabla_z f_1(z, b(\rho_s)) \cdot v_s(z) d\rho_s(z),$$

953 using the results from Lemma 20 for $\nabla_z \delta_\rho b[\rho_s]$, Assumption 1 and the fact that $Q(\rho)$ is constant in z and x , we
 954 have

$$\begin{aligned} L_2(\rho_s) &= - \iint [Q(\rho_s)^{-1} \nabla_x \nabla_z f_1(\tilde{z}, b(\rho_s)) \cdot v_s(\tilde{z})] \cdot \nabla_x \nabla_z f_1(z, b(\rho_s)) \cdot v_s(z) d\rho_s(z) d\rho_s(\tilde{z}) \\ &= - \langle u(\rho_s), Q(\rho_s)^{-1} u(\rho_s) \rangle \leq 0 \end{aligned}$$

955 Combining all terms together, we have that

$$\frac{d^2}{ds^2} G_b(\rho_s) \leq - \left(\alpha \tilde{\lambda} - \Lambda_1 \right) W_2(\rho_0, \rho_1)^2.$$

956 □

957 **Remark 9.** Under some additional assumptions on the functions f_1 and f_2 , we can obtain an improved
 958 convergence rate. In particular, assume that for all $z, x \in \mathbb{R}^d$,

959 • there exists a constant $\Lambda_2 \geq \lambda_2 \geq 0$ such that $\nabla_x^2 f_2(z, x) \preceq \Lambda_2 I_d$;

960 • there exists a constant $\sigma \geq 0$ such that $\|\nabla_x \nabla_z f_1(z, x)\| \geq \sigma$.

961 Then we have $-Q(\rho_s)^{-1} \preceq -1/(\beta + \Lambda_1 + \Lambda_2) \mathbf{I}_d$. Using Lemma 20, we then obtain a stronger bound on L_2
962 as follows:

$$\begin{aligned} L_2(\rho_s) &\leq -\frac{1}{\beta + \Lambda_1 + \Lambda_2} \|u(\rho_s)\|^2 \leq -\frac{1}{\beta + \Lambda_1 + \Lambda_2} \int \|\nabla_x \nabla_z f_1(z, b(\rho_s))\|^2 d\rho_s(z) \int \|v_s(z)\|^2 d\rho_s(z) \\ &\leq -\frac{\sigma^2}{\beta + \Lambda_1 + \Lambda_2} W_2(\rho_0, \rho_1)^2. \end{aligned}$$

963 This means we can improve the convergence rate in (26) to $\lambda_b := \alpha \tilde{\lambda} + \frac{\sigma^2}{\beta + \Lambda_1 + \Lambda_2} - \Lambda_1$.

964 **Proposition 22** (Ground state). *Let Assumptions 1-4 hold for $\alpha \tilde{\lambda} > \Lambda_1 \geq 0$ and $\beta > 0$. Then there exists*
965 *a unique maximizer ρ_* for the functional G_b over $\mathcal{P}(\mathbb{R}^d)$, and it satisfies $\rho_* \in \mathcal{P}_2(\mathbb{R}^d) \cap L^1(\mathbb{R}^d)$ and ρ_* is*
966 *absolutely continuous with respect to $\tilde{\rho}$.*

967 *Proof.* Uniqueness of the maximizer (if it exists) is guaranteed by the uniform concavity provided by Lemma 21.
968 To show existence of a maximizer, we use the direct method in the calculus of variations, requiring the
969 following key properties for G_b : (1) boundedness from above, (2) upper semi-continuity, and (3) tightness
970 of any minimizing sequence. To show (1), note that $\nabla_z^2(f_1(z, x) + \alpha \log \tilde{\rho}(z)) \preceq -(\alpha \tilde{\lambda} - \Lambda_1) \mathbf{I}_d$ for all
971 $z, x \in \mathbb{R}^d \times \mathbb{R}^d$ by Assumptions 2 and 4, and so

$$f_1(z, x) + \alpha \log \tilde{\rho}(z) \leq c_0(x) - \frac{(\alpha \tilde{\lambda} - \Lambda_1)}{4} |z|^2 \quad \forall (z, x) \in \mathbb{R}^d \times \mathbb{R}^d \quad (28)$$

972 with $c_0(x) := f_1(0, x) + \alpha \log \tilde{\rho}(0) + \frac{1}{\alpha \tilde{\lambda} - \Lambda_1} \|\nabla_z [f_1(0, x) + \alpha \log \tilde{\rho}(0)]\|^2$. Therefore,

$$\begin{aligned} G_b(\rho) &= \int [f_1(z, b(\rho)) + \alpha \log \tilde{\rho}(z)] d\rho(z) + \int f_2(z, b(\rho)) d\tilde{\rho}(z) + \frac{\beta}{2} \|b(\rho) - x_0\|^2 \\ &\quad - \alpha \int \rho \log \rho - \int \rho W * \rho \\ &\leq c_0(b(\rho)) + \int f_2(z, b(\rho)) d\tilde{\rho}(z) + \frac{\beta}{2} \|b(\rho) - x_0\|^2. \end{aligned}$$

973 To estimate each of the remaining terms on the right-hand side, denote $R := \|x_0\|^2 + \frac{2(\alpha_1 + \alpha_2)}{\beta}$ and recall that
974 $\|b(\rho)\| \leq R$ for any $\rho \in \mathcal{P}(\mathbb{R}^d)$ thanks to Lemma 18. By continuity of f_1 and $\log \tilde{\rho}$, there exists a constant
975 $c_1 \in \mathbb{R}$ such that

$$\sup_{x \in B_R(0)} c_0(x) = \sup_{x \in B_R(0)} \left[f_1(0, x) + \alpha \log \tilde{\rho}(0) + \frac{1}{\alpha \tilde{\lambda} - \Lambda_1} \|\nabla_z [f_1(0, x) + \alpha \log \tilde{\rho}(0)]\|^2 \right] \leq c_1. \quad (29)$$

976 The second term is controlled by c_2 thanks to Assumption 4. And the third term can be bounded directly to
977 obtain

$$G_b(\rho) \leq c_1 + c_2 + \beta(R^2 + \|x_0\|^2).$$

978 This concludes the proof of (1). Statement (2) was shown in Lemma 19. Then we obtain a minimizing sequence
979 $(\rho_n) \in \mathcal{P}(\mathbb{R}^d)$ which is in the closed unit ball of $C_0(\mathbb{R}^d)^*$ and so the Banach-Anaoglu theorem [Rud91, Theorem
980 3.15] there exists a limit ρ_* in the Radon measures and a subsequence (not relabeled) such that $\rho_n \xrightarrow{*} \rho_*$. In fact,
981 ρ_* is absolutely continuous with respect to $\tilde{\rho}$ as otherwise $G_b(\rho_*) = -\infty$, which contradicts that $G_b(\cdot) > -\infty$
982 somewhere. We conclude that $\rho_* \in L^1(\mathbb{R}^d)$ since $\tilde{\rho} \in L^1(\mathbb{R}^d)$ by Assumption 2. To ensure $\rho_* \in \mathcal{P}(\mathbb{R}^d)$,
983 we require (3) tightness of the minimizing sequence (ρ_n) . By Markov's inequality [Gho02] it is sufficient to
984 establish a uniform bound on the second moments:

$$\int \|z\|^2 d\rho_n(z) < C \quad \forall n \in \mathbb{N}. \quad (30)$$

985 To see this we proceed in a similar way as in the proof of Proposition 10. Defining

$$K(\rho) := - \int [f_1(z, b(\rho)) + \alpha \log \tilde{\rho}(z)] d\rho(z) + \alpha \int \rho \log \rho dz + \frac{1}{2} \int \rho W * \rho dz,$$

986 we have $K(\rho) = -G_b(\rho) + \int f_2(z, b(\rho)) d\tilde{\rho}(z) + \frac{\beta}{2} \|b(\rho) - x_0\|^2$. Then using again the bound on $b(\rho)$ from
987 Lemma 18,

$$\begin{aligned} K(\rho) &\leq -G_b(\rho) + \sup_{x \in B_R(0)} \int f_2(z, x) d\tilde{\rho}(z) + \beta (R^2 + \|x_0\|^2) \\ &\leq -G_b(\rho) + c_2 + \beta (R^2 + \|x_0\|^2), \end{aligned}$$

988 where the last inequality is thanks to Assumption 4. Hence, using the estimates (28) and (29) from above, and
 989 noting that the sequence (ρ_n) is minimizing $(-G_b)$, we have

$$\begin{aligned} \frac{(\alpha\tilde{\lambda} - \Lambda_1)}{4} \int \|z\|^2 d\rho_n(z) &\leq c_0(b(\rho_n)) - \int [f_1(z, b(\rho_n)) + \alpha \log \tilde{\rho}(z)] d\rho_n(z) \\ &\leq c_1 + K(\rho_n) \leq c_1 - G_b(\rho_n) + c_2 + \beta (R^2 + \|x_0\|^2) \\ &\leq c_1 - G_b(\rho_1) + c_2 + \beta (R^2 + \|x_0\|^2) < \infty. \end{aligned}$$

990 which uniformly bounds the second moments of (ρ_n) . This concludes the proof for the estimate (30) and also
 991 ensures that $\rho_* \in \mathcal{P}_2(\mathbb{R}^d)$. \square

992 **Corollary 23.** *Any maximizer ρ_* of G_b is a steady state for equation (4) according to Definition 9, and satisfies*
 993 $\text{supp}(\rho_*) = \text{supp}(\tilde{\rho})$.

994 *Proof.* To show that ρ_* is a steady state we can follow exactly the same argument as in the proof of Corollary 12,
 995 just replacing $-\frac{1}{\alpha} \int f_1(z, x) \mu_*(x)$ with $+\frac{1}{\alpha} \int f_1(z, b(\rho_*))$. It remains to show that $\text{supp}(\rho_*) = \text{supp}(\tilde{\rho})$. As
 996 ρ_* is a maximizer, it is in particular a critical point, and therefore satisfies that $\delta_\rho G_b[\rho_*](z)$ is constant on all
 997 connected components of $\text{supp}(\rho_*)$. Thanks to Lemma 17, this means there exists a constant $c[\rho_*]$ (which may
 998 be different on different components of $\text{supp}(\rho_*)$) such that

$$f_1(z, b(\rho_*)) - \alpha \log \left(\frac{\rho_*(z)}{\tilde{\rho}(z)} \right) - W * \rho_*(z) = c[\rho_*] \quad \text{on } \text{supp}(\rho_*).$$

999 Rearranging, we obtain (for a possible different constant $c[\rho_*] \neq 0$)

$$\rho_*(z) = c[\rho_*] \tilde{\rho}(z) \exp \left[\frac{1}{\alpha} (f_1(z, b(\rho_*)) - W * \rho_*(z)) \right] \quad \text{on } \text{supp}(\rho_*). \quad (31)$$

1000 Firstly, note that $\text{supp}(\rho_*) \subset \text{supp}(\tilde{\rho})$ since ρ_* is absolutely continuous with respect to $\tilde{\rho}$. Secondly, note
 1001 that $\exp \frac{1}{\alpha} f_1(z, b(\rho_*)) \geq 1$ for all $z \in \mathbb{R}^d$ since $f_1 \geq 0$. Finally, we claim that $\exp(-\frac{1}{\alpha} W * \rho_*(z)) > 0$ for
 1002 all $z \in \mathbb{R}^d$. In other words, we claim that $W * \rho_*(z) < \infty$ for all $z \in \mathbb{R}^d$. This follows by exactly the same
 1003 argument as in Corollary 12, see equation (19). We conclude that $\text{supp}(\rho_*) = \text{supp}(\tilde{\rho})$. \square

1004 **Remark 10.** *If we have in addition that $\tilde{\rho} \in L^\infty(\mathbb{R}^d)$ and $f_1(\cdot, x) \in L^\infty(\mathbb{R}^d)$ for all $x \in \mathbb{R}^d$, then the*
 1005 *maximizer ρ_* of G_b is in $L^\infty(\mathbb{R}^d)$ as well. This follows directly by bounding the right-hand side of (31).*

1006 With the above preliminary results, we can now show the HWI inequality, which implies again a Talagrand-type
 1007 inequality and a generalized logarithmic Sobolev inequality.

1008 **Proposition 24** (HWI inequalities). *Define the dissipation functional*

$$D_b(\gamma) := \iint |\delta_\rho G_b[\rho](z)|^2 d\rho(z).$$

1009 *Assume $\alpha, \beta > 0$ such that $\alpha\tilde{\lambda} > \Lambda_1 + \sigma^2$, and let λ_b as defined in (26). Denote by ρ_* the unique maximizer of*
 1010 G_b .

1011 **(HWI)** *Let $\rho_0, \rho_1 \in \mathcal{P}_2(\mathbb{R}^d)$ such that $G_b(\rho_0), G_b(\rho_1), D_b(\rho_0) < \infty$. Then*

$$G_b(\rho_0) - G_b(\rho_1) \leq \overline{W}(\rho_0, \rho_1) \sqrt{D_b(\rho_0)} - \frac{\lambda_b}{2} W_2(\rho_0, \rho_1)^2 \quad (32)$$

1012 **(logSob)** *Any $\rho \in \mathcal{P}_2(\mathbb{R}^d)$ such that $G(\rho), D_b(\rho) < \infty$ satisfies*

$$D_b(\rho) \geq 2\lambda_b G_a(\rho | \rho_*). \quad (33)$$

1013 **(Talagrand)** *For any $\rho \in \mathcal{P}_2(\mathbb{R}^d)$ such that $G_b(\rho) < \infty$, we have*

$$W_2(\rho, \rho_*)^2 \leq \frac{2}{\lambda_b} G_b(\rho | \rho_*). \quad (34)$$

1014 *Proof.* The proof for this result follows analogously to the arguments presented in the proofs of Proposition 13,
 1015 Corollary 14 and Corollary 15, using the preliminary results established in Proposition 21 and Proposition 22. \square

1016 *Proof of Theorem 2.* Following the same approach as in the proof of Theorem 1, the results in Theorem 2
 1017 immediately follow by combining Proposition 22, Corollary 23 and Proposition 24 applied to solutions of the
 1018 PDE (4). \square

1019 **D Proof of Theorem 3**

The proof for this theorem uses similar strategies as that of Theorem 2, but is simpler due to the evolution reducing to an ODE rather than a PDE. Recall that for any $x \in \mathbb{R}^d$ the best response $r(x)(\cdot) \in \mathcal{P}(\mathbb{R}^d)$ in (5) is defined as

$$r(x) := \operatorname{argmin}_{\hat{\rho} \in \mathcal{P}} -G_c(\hat{\rho}, x).$$

1020

1021 **Lemma 25.** *Let Assumptions 3 and 4 hold. Then for each $x \in \mathbb{R}^d$ there exists a unique maximizer $\rho_* := r(x)$*
 1022 *solving $\operatorname{argmax}_{\hat{\rho} \in \mathcal{P}_2} G_c(\hat{\rho}, x)$.*

1023 *Proof.* Equivalently, consider the minimization problem for $F(\rho) = -\int f_1(z, x) d\rho(z) + \alpha KL(\rho | \tilde{\rho}) +$
 1024 $\frac{1}{2} \int \rho W * \rho$ with some fixed x . Note that we can rewrite $F(\rho)$ as

$$F(\rho) = \int \rho \log \rho dz + \int V(z) d\rho(z) + \frac{1}{2} \int \rho W * \rho$$

1025 where $V(z) := -(f_1(z, x) + \alpha \log \tilde{\rho}(z))$ is convex by Assumption 4. Together with Assumption 3, we can
 1026 directly apply the uniqueness and existence result from [CMV03, Theorem 2.1 (i)]. \square

1027 The best response function $r(x)$ is supported on the whole of \mathbb{R}^d thanks to the diffusion term $\int \rho \log \rho$ in G_c ,
 1028 and there exists a function $c : \mathbb{R}^d \mapsto \mathbb{R}$ such that $r(x)(z)$ solves the Euler-Lagrange equation

$$\delta_\rho G_c[\rho, x](z) := \alpha \log \rho(z) - (f_1(z, x) + \alpha \log \tilde{\rho}(z)) + (W * \rho)(z) = c(x) \quad \text{for all } (z, x) \in \mathbb{R}^d \times \mathbb{R}^d. \quad (35)$$

1029 **Lemma 26.** *Let $r(x)$ as defined in (5). If $r \in C^1(\mathbb{R}^d; \mathcal{P}(\mathbb{R}^d))$, then we have $\nabla_x G_d(x) =$*
 1030 *$(\nabla_x G_c(\rho, x))|_{\rho=r(x)}$.*

1031 *Proof.* We start by computing $\nabla_x G_d(x)$. We have

$$\begin{aligned} \nabla_x G_d(x) &= \nabla_x (G_c(r(x), x)) = \int \delta_\rho [G_c(\rho, x)]|_{\rho=r(x)}(z) \nabla_x r(x)(z) dz + (\nabla_x G_c(\rho, x))|_{\rho=r(x)} \\ &= c(x) \nabla_x \int r(x)(z) dz + (\nabla_x G_c(\rho, x))|_{\rho=r(x)} = (\nabla_x G_c(\rho, x))|_{\rho=r(x)}, \end{aligned}$$

1032 where we used that $r(x)$ solves the Euler-Lagrange equation (35) and that $r(x) \in \mathcal{P}(\mathbb{R}^d)$ for any $x \in \mathbb{R}^d$ so
 1033 that $\int r(x)(z) dz$ is independent of x . \square

1034 **Remark 11.** *By showing suitable bounds on the second derivative of $G_d(x)$, the regularity assumption on $r(x)$*
 1035 *can be removed following the approach in [Liu+21].*

1036 **Lemma 27.** *Let Assumption 1 hold. Then $G_d : \mathbb{R}^d \rightarrow \mathbb{R} \cup \{+\infty\}$ is strongly convex with constant $\lambda_d :=$*
 1037 *$\lambda_1 + \lambda_2 + \beta > 0$.*

1038 *Proof.* The energy $G_c(\rho, x)$ is strongly convex in x due to our assumptions on f_1, f_2 , and the regularizing term
 1039 $\|x - x_0\|_2^2$. This means that for any $\rho \in \mathcal{P}$,

$$G_c(\rho, x) \geq G_c(\rho, x') + \nabla_x G_c(\rho, x')^\top (x - x') + \frac{\lambda_d}{2} \|x - x'\|_2^2.$$

1040 Selecting $\rho = r(x')$, we have

$$G_c(r(x'), x) \geq G_c(r(x'), x') + \nabla_x G_c(r(x'), x')^\top (x - x') + \frac{\lambda_d}{2} \|x - x'\|_2^2.$$

1041 Since $G_c(r(x'), x) \leq G_c(r(x), x)$ by definition of $r(x)$, we obtain the required convexity condition:

$$G_d(x) = G_c(r(x), x) \geq G_c(r(x'), x') + \nabla_x G_c(r(x'), x')^\top (x - x') + \frac{\lambda_d}{2} \|x - x'\|_2^2.$$

1042 \square

1043 *Proof of Theorem 3.* For any reference measure $\rho_0 \in \mathcal{P}$, we have

$$G_d(x) \geq G_c(\rho_0, x) \geq -\alpha KL(\rho_0 | \tilde{\rho}) - \frac{1}{2} \int \rho_0 W * \rho_0 + \frac{\beta}{2} \|x - x_0\|_2^2$$

1044 and therefore, G_d is coercive. Together with the strong convexity provided by Lemma 27, we obtain the existence
 1045 of a unique minimizer $x_\infty \in \mathbb{R}^d$. Convergence in norm now immediately follows also using Lemma 27: for
 1046 solutions $x(t)$ to (5), we have

$$\frac{1}{2} \frac{d}{dt} \|x(t) - x_\infty\|^2 = -(G_d(x(t)) - G_d(x_\infty)) \cdot (x(t) - x_\infty) \leq -\lambda_d \|x(t) - x_\infty\|^2.$$

1047 A similar result holds for convergence in entropy using the Polyák-Łojasiewicz convexity inequality

$$\frac{1}{2} \|\nabla G_d(x)\|_2^2 \geq \lambda_d (G_d(x) - G_d(x_\infty)),$$

1048 which is itself a direct consequence of strong convexity provided in Lemma 27. Then

$$\frac{d}{dt} (G_d(x(t)) - G_d(x_\infty)) = \nabla_x G_d(x(t)) \cdot \dot{x}(t) = -\|\nabla_x G_d(x(t))\|^2 \leq -2\lambda_d (G_d(x(t)) - G_d(x_\infty)),$$

1049 and so the result in Theorem 3 follows. \square

1050 E Additional Simulation Results

1051 We simulate a number of additional scenarios to illustrate extensions beyond the setting with provable guarantees
 1052 and in the settings for which we have results but no numerical implementations in the main paper. First, we
 1053 simulate the aligned objectives setting in one dimension, corresponding to (3). Then we consider two settings
 1054 which are not covered in our theory: (1) the previously-fixed distribution $\tilde{\rho}$ is also time varying, and (2) the
 1055 algorithm does not have access to the full distributions of ρ and $\tilde{\rho}$ and samples from them to update. Lastly, we
 1056 illustrate a classifier with the population attributes in two dimensions, which requires a different finite-volume
 1057 implementation [CCH15, Section 2.2] than the one dimension version of the PDE due to flux in two dimensions.

1058 E.1 Aligned Objectives

1059 Here we show numerical simulation results for the aligned objectives case, where the population and distribution
 1060 have the same cost function. In this setting, the dynamics are of the form

$$\begin{aligned} \partial_t \rho &= \operatorname{div}(\rho \nabla_z \delta_\rho G_a[\rho, \mu]) \\ &= \operatorname{div}\left(\rho \nabla_z \left(\int f_1(z, x) d\mu(x) + \alpha \log(\rho/\tilde{\rho}) + W * \rho\right)\right) \\ \frac{d}{dt} x &= -\nabla_x \left(\int f_1(z, x) d\rho(z) + \int f_2(z, x) d\tilde{\rho}(z) + \frac{\beta}{2} \|x - x_0\|^2\right) \end{aligned}$$

1061 where f_1 and f_2 are as defined in section 4.1, and $W = \frac{1}{20}(1+z)^{-1}$, a consensus kernel. Note that W does
 1062 not satisfy Assumption 3, but we still observe convergence in the simulation. This is expected; in other works
 1063 such as [CMV03], the assumptions on W are relaxed and convergence results proven given sufficient convexity
 1064 of other terms. The regularizer $\tilde{\rho}$ is set to ρ_0 , which models a penalty for the effort required of individuals to
 1065 alter their attributes. The coefficient weights are $\alpha = 0.1$ and $\beta = 1$, with discretization parameters $dz = 0.1$,
 1066 $dt = 0.01$.

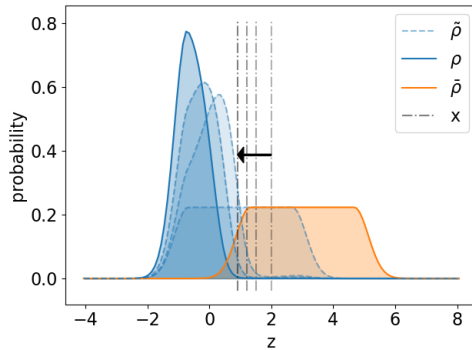


Figure 4: The dynamics include a consensus kernel, which draws neighbors in z -space closer together. We see that the population moves to make the classifier performer better, as the two distributions become more easily separable by the linear classifier.

1067 In Figure 4, we observe the strategic distribution separating itself from the stationary distribution, improving
 1068 the performance of the classifier and also improving the performance of the population itself. The strategic
 1069 distribution and classifier appear to be stationary by time $t = 40$.

1070 **E.2 Multiple Dynamical Populations**

1071 We also want to understand the dynamics when both populations are strategic and respond to the classifier. In
 1072 this example, we numerically simulate this and in future work we hope to prove additional results regarding
 1073 convergence. This corresponds to modeling the previously-fixed distribution $\bar{\rho}$ as time-dependent; let this
 1074 distribution be $\tau \in \mathcal{P}_2$. We consider the case where ρ is competitive with x and τ is aligned with x , with
 1075 dynamics given by

$$\begin{aligned} \partial_t \rho &= -\operatorname{div}(\rho \nabla_z (f_1(z, x) - \alpha \log(\rho/\bar{\rho}) - W * \rho)) \\ \partial_t \tau &= \operatorname{div}(\tau \nabla_z (f_2(z, x) + \alpha \log(\tau/\bar{\tau}) + W * \tau)) \\ \frac{d}{dt} x &= -\nabla_x \left(\int f_1(z, x) d\rho(z) + \int f_2(z, x) d\tau(z) + \frac{\beta}{2} \|x - x_0\|^2 \right). \end{aligned}$$

We use $W = 0$ and f_1, f_2 as in section 4.1 and the same discretization parameters as in Section E.1. In Figure 5,

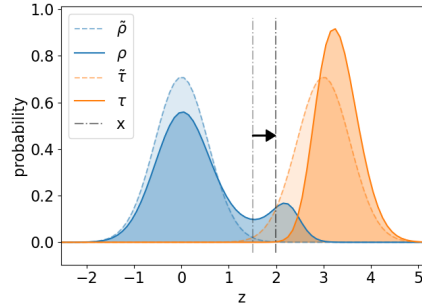


Figure 5: The population ρ aims to be classified with the τ population, while the classifier moves to delineate between the two. We observe that τ adjusts to improve the performance of the classifier while ρ competes against it. The distributions are plotted at time $t = 0$, corresponding to $\bar{\rho}$ and $\bar{\tau}$, and time $t = 20$, corresponding to ρ and τ .

1076 we observe that the τ population moves to the right, assisting the classifier in maintaining accurate scoring.
 1077 In contrast, ρ also moves to the right, rendering the right tail to be classified incorrectly, which is desirable
 1078 for individuals in the ρ population but not desirable for the classifier. While we leave analyzing the long-term
 1079 behavior mathematically for future work, the distributions and classifier appear to converge by time $t = 20$.
 1080

1081 **E.3 Sampled Gradients**

1082 In real-world applications of classifiers, the algorithm may not know the exact distribution of the population,
 1083 relying on sampling to estimate it. In this section we explore the effects of the classifier updating based on an
 1084 approximated gradient, which is computed by sampling the true underlying distributions ρ and $\bar{\rho}$. We use the
 1085 same parameters for the population dynamics as in section 4.1, and for the classifier we use the approximate
 1086 gradient

$$\nabla_x L(z, x_t) \approx \sum_{i=1}^n \nabla_x f_1(z_i, x_t) + \nabla_x f_2(\bar{z}_i, x_t) + \beta(x_t - x_0), \quad z_i \sim \rho_t, \quad \bar{z}_i \sim \bar{\rho}_t.$$

1087 First, we simulate the dynamics with the classifier and the strategic population updating at the same rate, using
 1088 $\alpha = 0.05$, $\beta = 1$, and the same consensus kernel as used previously, with the same discretization parameters as
 1089 in E.1. In Figure 6, we observe no visual difference between the two results with $n = 4$ versus $n = 40$ samples,
 1090 which suggests that not many samples are needed to estimate the gradient.

1091 Next, we consider the setting where the classifier is best-responding to the strategic population.

1092 Unlike the first setting, we observe in Figure 7 a noticeable difference between the evolution of ρ_t with $n = 4$
 1093 versus $n = 40$ samples. This is not surprising because optimizing with a very poor estimate of the cost function
 1094 at each time step would cause x_t to vary wildly, and this method fails to take advantage of correct "average"
 1095 behavior that gradient descent provides.

1096 **E.4 Two-dimensional Distributions**

1097 In practice, individuals may alter more than one of their attributes in response to an algorithm, for example, both
 1098 cancelling a credit card and also reporting a different income in an effort to change a credit score. We model this

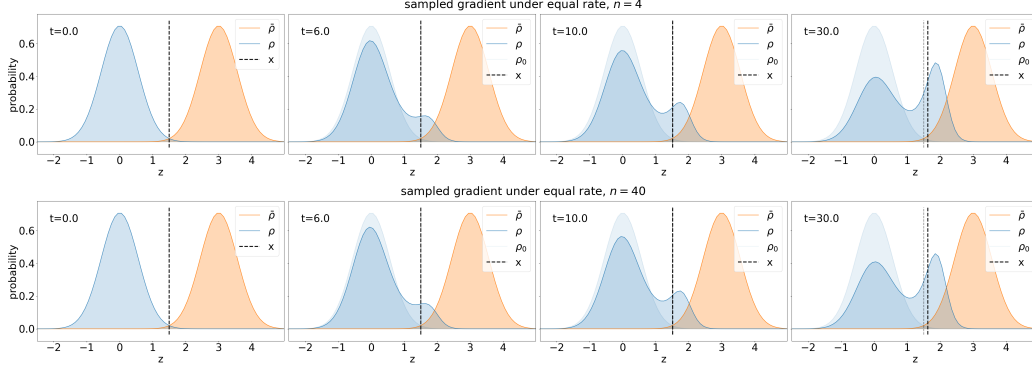


Figure 6: When the classifier is updating at the same rate as the population, we do not see a significant change in the evolution of both species, suggesting that as long as the gradient estimate for the classifier is correct on average, the estimate itself does not need to be particularly accurate.

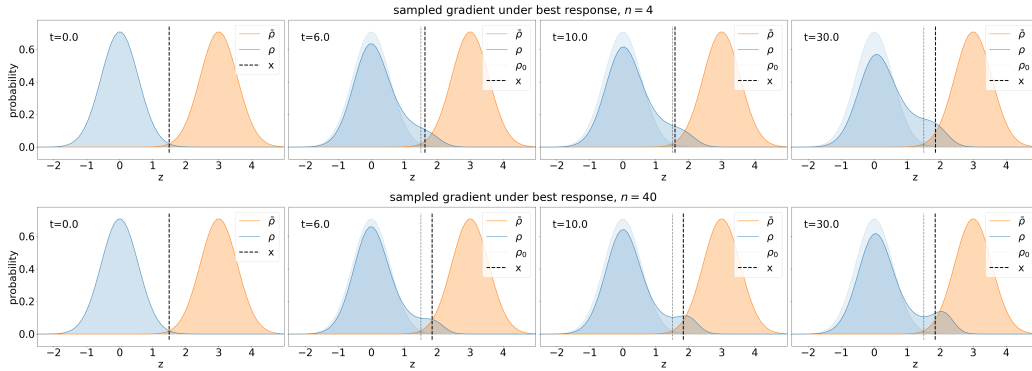


Figure 7: When the classifier is best-responding to the population, we observe that using $n = 4$ samples leads to different behavior for both the classifier and the population, compared with a more accurate estimate using $n = 40$ samples.

1099 case with $z \in \mathbb{R}^2$ and $x \in \mathbb{R}^2$, and simulate the results for the setting where the classifier and the population
 1100 are evolving at the same rate. While this setting is not covered in our theory, it interpolates between the two
 1101 timescale extremes.

1102 We consider the following classifier:

$$\begin{aligned} f_1(z, x) &= \frac{1}{2} \left(1 - \frac{1}{1 + \exp x^\top z} \right) \\ f_2(z, x) &= \frac{1}{2} \left(\frac{1}{1 + \exp x^\top z} \right) \end{aligned} \quad (36)$$

1103 with $W = 0$. Again, the reference distribution $\tilde{\rho}$ corresponds to the initial shape of the distribution, instituting
 1104 a penalty for deviating from the initial distribution. We use $\alpha = 0.5$ and $\beta = 1$ for the penalty weights, run
 1105 for $t = 4$ with $dt = 0.005$ and $dx = dy = 0.2$ for the discretization. In this case, the strategic population is
 1106 competing with the classifier, with dynamics given by

$$\begin{aligned} \partial_t \rho &= -\operatorname{div}(\rho \nabla_z (f_1(z, x) - \alpha \log(\rho/\tilde{\rho}))) \\ \frac{d}{dt} x &= -\nabla_x \left(\int f_1(z, x) d\rho(z) + \int f_2(z, x) d\tilde{\rho}(z) + \frac{\beta}{2} \|x - x_0\|^2 \right) \end{aligned}$$

1107 In Figure 8, we observe the strategic population increasing mass toward the region of higher probability of being
 1108 labeled "1" while the true underlying label is zero, with the probability plotted at time $t = 4$. This illustrates
 1109 similar behavior to the one-dimensional case, including the distribution splitting into two modes, which is
 1110 another example of polarization induced by the classifier. Note that while in this example, $x \in \mathbb{R}^2$ and we use a
 1111 linear classifier; we could have $x \in \mathbb{R}^d$ with $d > 2$ and different functions for f_1 and f_2 which yield a nonlinear
 1112 classifier; our theory in the timescale-separated case holds as long as the convexity and smoothness assumptions
 1113 on f_1 and f_2 are satisfied.

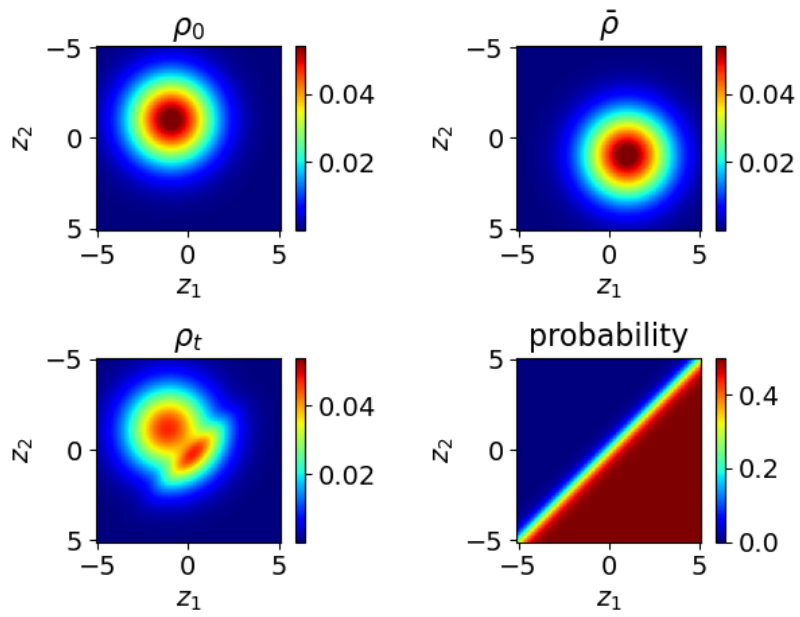


Figure 8: We use (36) for the classifier functions, using a Gaussian initial condition and regularizer for ρ . We see the distribution moving toward the region with higher probability of misclassification.